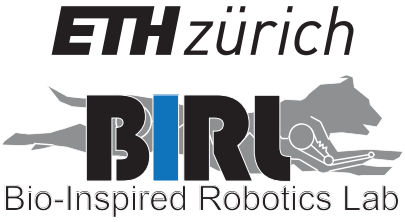

Master-Thesis

Design and Control of an Active Tail for Robot Locomotion

An evaluation for use and design of an active tail for steady-state locomotion in the sagittal plane.

Spring Term 2014

Supervised by:

Mostafa Ajallooeian

Peter Eckert

Massimo Vespignani

Prof. Fumiya Iida

Prof. Auke Ijspeert

Author:

Steve W. Heim

Abstract

In this thesis we explore the use of a tail for terrestrial locomotion of animals and robots. We focus on steady-state locomotion in the sagittal plane over smooth terrain, with an emphasis on the exploitation of natural dynamics. We approach the problem in three ways:
first we analyze the equations of motion to find the effect on the dynamics of the control input associated with the tail. From this we hypothesize that the tail's primary function is to stabilize body pitch, and more importantly that the system's morphology should be optimized in such a way that the control task of body-pitch stabilization is decoupled from the task of energy-input. We also explore the implications of scaling and compare this with a few cases in biology.
Second we run optimizations on the derived models to find open-loop periodic solutions. We optimize over both the control inputs as well as morphological parameters. We thus observe if the optimal solutions match with the predictions from our previous hypothesis, as well as the effect of different cost functions.
Third, we have built a simple 1 degree of freedom tail and tested it's use in finding a bounding gait with the Cheetah-Cub robot developed at the BioRob lab at EPFL. With this robot we have empirically tested the effect of different tail-parameters such as size and weight, as well as determined the importance of the patterns for a Central Pattern Generator (CPG) to generate open-loop inputs to synthesize stable bounding.
By matching the results in all three approaches we shed some light on the opportunities in which incorporating a tail in a robot makes sense, as well as suggest some reasons why most large land animals do not use tails for locomotion.

Acknowledgements

I would like to thank my tutor at ETHZ, professor Fumiya Iida, for advising and giving me the opportunity of completing my master thesis at the BioRob lab at EPFL. Professor Iida has always been friendly and accessible during my entire studies, as well as very encouraging in broadening the scope of my studies and ways of looking at research.
I would also like to thank professor Auke Ijspeert of the BioRob lab at EPFL. Professor Ijspeert was also very encouraging as well as very welcoming, never hesitating to include me in the going-ons of the lab. Due to his generosity I also had the opportunity to meet and talk to other high-profile researchers in the field.

During this thesis I had the fortune of having not just one supervisor, but three: Mostafa Ajallooeian, Peter Eckert and Massimo Vespignani. All three not only gave me good advice, but became good friends over the course of the semester.
Mostafa's calm demeanor yet never-ending humor and philosophical questions were a welcome respite from long days of staring at a computer screen. His serious and rigorous approach also provided a guideline and the motivation to aim farther than the thesis itself and actually push for a publication.
Peter's guidance managed to strike the fine balance between ensuring I got everything working in time and at the same time letting me explore my own ideas and make enough mistakes that I would learn things the lasting way. Despite his own pressing schedule, he always kept tabs on me and made sure to prod me when I started slacking, then allow me an open road once I picked up momentum.
Because of Massimo's easy-going friendliness, combined with very down-to-earth advice on how to approach problems as well as when to simply avoid them, he was often the first person I went to for advice and assistance. His encouragement led me to committing to explore also the biological relevance of the tail, which eventually led to the SICB conference.
Two more people were very directly involved in the project: François Longchamp, the mechanical technician of BioRob, and Daniel Chapuis, a CAD designer interning at BioRob. François Longchamp redesigned the legs of the Cheetah-Cub and took care of all the manufacturing of parts, while Daniel took care of the CAD design for the parts. Both gave me valuable advice during the conceptual phase, and what is more, were very easy to talk to and work with. During the second half of the thesis, François even put in extra hours to get the new version of Cheetah-Cub ready in time for me to still use it for my tests, and Daniel cheerfully endured through my endless whims on small adjustments to designs.

I also often received valuable advice from the rest of the lab. This has been one of the most cheerful, welcoming and helpful group of people I've had the pleasure to work with, and I hope to have the opportunity to collaborate with them all again.

Finally, I would like to thank professor Robert Full of the PolyPedal lab at Berkeley who, despite never having met me, graciously agreed to sponsor my submission of the results of this thesis to the SICB conference.

Symbols

x	Body horizontal displacement
y	Body vertical displacement
φ	Body pitch angle
y_F	Leg extension
φ_H	Hip angle
φ_T	Tail angle
q	Vector of displacement variables
$M_{(q)}$	Mass matrix
$H_{(q,\dot{q})}$	Vector of differentiable forces
$B_{(q)}$	Control matrix
$J^{\intercal}_{c(q)}$	Contact Jacobian
λ_{GRF}	Ground Reaction Forces
F	Force
τ	Torque
g	Gravity
d	Distance
m	Mass
V	Volume
J	Moment of inertia
l	Length
k	Spring coefficient
k_0	Spring resting length
b	damping coefficient
ρ	density
f_{stride}	stride frequency
a_n and b_n	Fourier coefficients
$\mathbf{x}$	Vector of state variables
K_x	Motor constant
R	Resistance
α_1, α_2, α_{31} and α_{32}	Tail effectiveness coefficients

Acronyms and Abbreviations

EPFL	École Polytechnique Fédérale de Lausanne
BioRob	Biorobotics Laboratory, EPFL
ETHZ	Eidgenössische Technische Hochschule Zürich
BIRL	Bio-Inspired Robotics Laboratory, ETHZ
CoT	Cost of Transport
Fr	Froude number
EoM	Equations of Motion
DoF	Degrees of Freedom
MoI	Moment of Inertia
GRF	Ground Reaction Force
SLIP	Spring-Loaded Inverted Pendulum
CPG	Central Pattern Generator
ZMP	Zero Moment Point
AoA	Angle of Attack
PSO	Particle Swarm Optimization
IMU	Inertial Measurement Unit

Contents

Chapter 1

Introduction

Before entering in the actual work of this thesis, we briefly present the field of bio-inspired robotics and legged-locomotion to help the reader better understand the motivation, scientific background, state-of-the-art as well as some historical context of this thesis. In this thesis, we focus on the role of tails in steady-state legged locomotion. What we gleam on the topic can help understand how to build better robots as well as better understand how tails are used by animals. During the thesis, we've approached the topic with a mathematical analysis of the dynamics using an abstracted model, performed optimizations in simulation to find qualitative results, as well as built a simple 1 degree-of-freedom (DoF) tail to quantitative experiments on the BioRob lab's cheetah-cub robot[44]. Before going more into detail on this however, it will be helpful for the reader to be introduced to some background of the field, which will be covered in the rest of this chapter.

1.1 Nature and Engineering

Humans have always been inspired by nature, not only for artistic pursuits but also in engineering endeavors. Indeed until the advent of modern universities around the 19TH century, people did not tend to specialize in a single field: instead they would be engineers, philosophers, artists, physicians, mathematicians and even politicians all at the same time. Perhaps one of the most known and epitomized examples is *Leonardo da Vinci* (1452-1519) who, while being primarily famous as an artist and engineer, was indeed a polymath and worked also in philosophy, botany, mathematics and many other fields. Amongst his most well known designs are his flying contraptions, including an ornithopter inspired by bird wings. Whilst designing these flying machines, he closely studied nature for inspiration, writing also a manuscript on the subject, the *Codex on the Flight of Birds*. Although da Vinci never succeeded in building a manned flying machine, in his codex he does observe that in birds the center of pressure does not coincide with the center of gravity, as shown in the sketch of figure 1.1, a well known concept which is regularly employed nowadays in the design of aircraft and rockets.

This shows an early direct example of searching for engineering solutions by studying animals. This concept has even been extended to use in legged-robotics[1][36].

Conversely, the case of photographic studies of locomotion performed by *Ètienne-Jules Marey* (1830-1904) and *Eadweard Muybridge* (1830-1904) is an excellent example of the advancement of technical methods for the purpose of understanding nature. During their time, the presence of a flight-phase during running gaits was a much debated topic, with both opponents and proponents. Though Marey allegedly stated it already in his 1873 publication *La Machine Animale*[29], it

[1] I have found no publication of it yet, however Jerry Pratt discussed using the concept of buoyancy from boats in high-speed running at Dynamic Walking 2014.

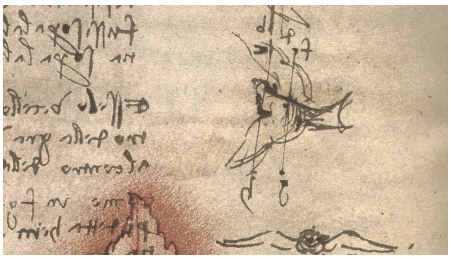

Figure 1.1: A sketch from Da Vinci's "Codex on the Flight of Birds", illustrating the center of pressure. A beautiful scan of the entire work as well as English translation can be found at website of the Smithsonian National Air and Space Museum (where this sketch was taken). http://airandspace.si.edu/exhibitions/codex/

was Muybridge to become famous for finally proving this via a series of high-speed photographs, see figure 1.2 which clearly showed this flight-phase.

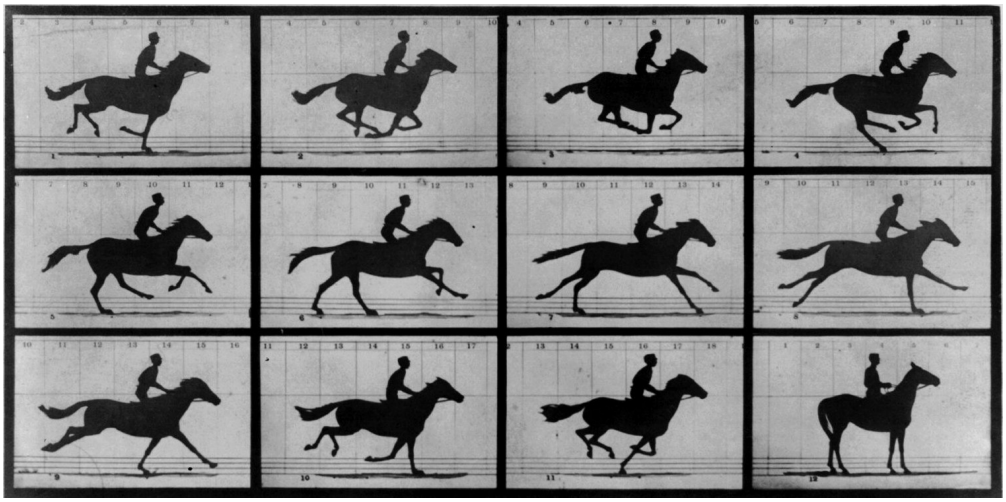

Figure 1.2: Muybridge photographically captured the various phases of horses running via a battery of sixteen photo-apparatuses hooked up to tripwires buried in the racetrack. These photographs helped convince the general public that running involved a *flight phase* during which the entire body is in the air.

However, Marey's work had a far more significant, if less well-known, impact on the scientific approach to animal locomotion. A physician and not a photographer by training, Marey's primary fascination was understanding the principles of movement. Whilst Muybridge frequently doctored his images or even composed sequences with images taken during different runs in order to obtain a visually more appealing end-product, Marey was scrupulous in his efforts to make reproduceable and quantifiable photographic measurements. When constructing his chronophotographic setups, he paid much attention to being able to precisely define the time intervals between each shot, often synchronizing the photographs with measurements from other devices. In his studio he conducted studies with multiple exposures on the same plate which clearly illustrate various phases of dynamic motion (see figure 1.3). In order to remove distractions, test-subjects were sometimes required to wear black suits with markers on their limbs (see figure, so that only the segments representing each limb were exposed on the photography, in a manner not dissimilar to modern motion-capture technology albeit in 2-D.
In further studies Marey even classified gaits while taking into account energetics and ground

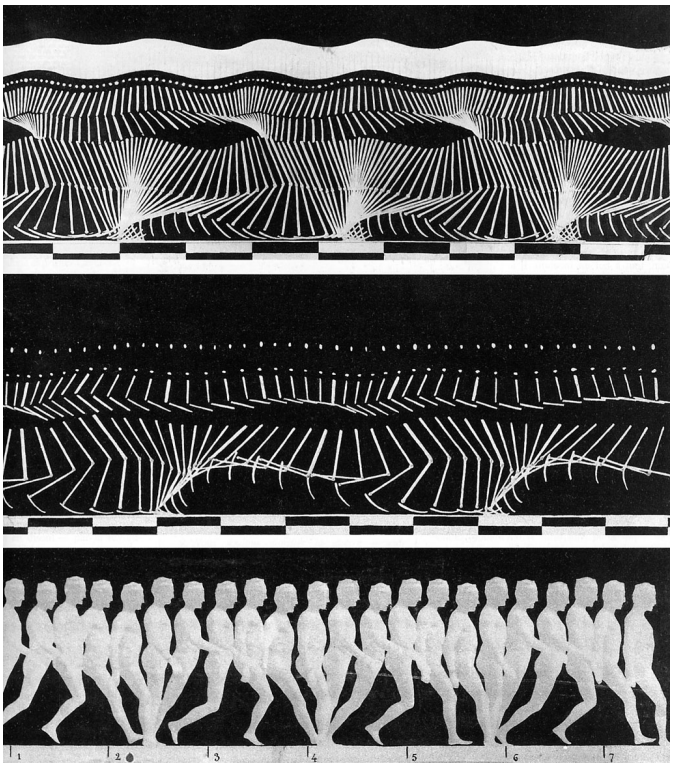

Figure 1.3: In order to isolate the movements of individual limbs, Marey's subjects would wear black suits marked with white lines. A rapid sequence of exposures at regular intervals thus revealed the joint motions through a stride.

reaction forces, building an ad-hoc myograph and pressure-sensitive shoes. Though these measurements were far from precise, they already allowed Marey to classify gaits by foot-fall pattern and duration of stance (see figure 1.4). In contrast to many of his contemporaries, Marey made heavy use of highly technical methods in his studies, even pushing the limits of what was then possible: his extensive work on high-speed photography and animating motion was for him just an ends to studying biology, nonetheless it was fundamental to the continuing work of the Lumière brothers in cinematography. Perhaps more importantly, Marey's adoption of more systematic and quantifiable methods to study and classify motion in animals paved the way towards a more mathematical, analytical approach to the field.
Recently bio-mimetics, bio-inspiration and bio-robotics have become very popular buzz-words, however Da Vinci and Marey exemplify the fact that the exchange between nature and engineering has been continuous and ever-present.

1.2 Legged Locomotion

1.2.1 Legged Locomotion in Nature

Unlike the solutions introduced in the previous subsection, in nature locomotion doesn't rely exclusively on a central controller (i.e. the brain) for solving complex coordination and stability problems. In the 1970s experiments on decerebrate cats[2] revealed that the cats were capable of actually changing between gaits with completely different footfall patterns, proving the brain does

[2] *Decerebration* is the process of removing cerebral brain function in an animal.

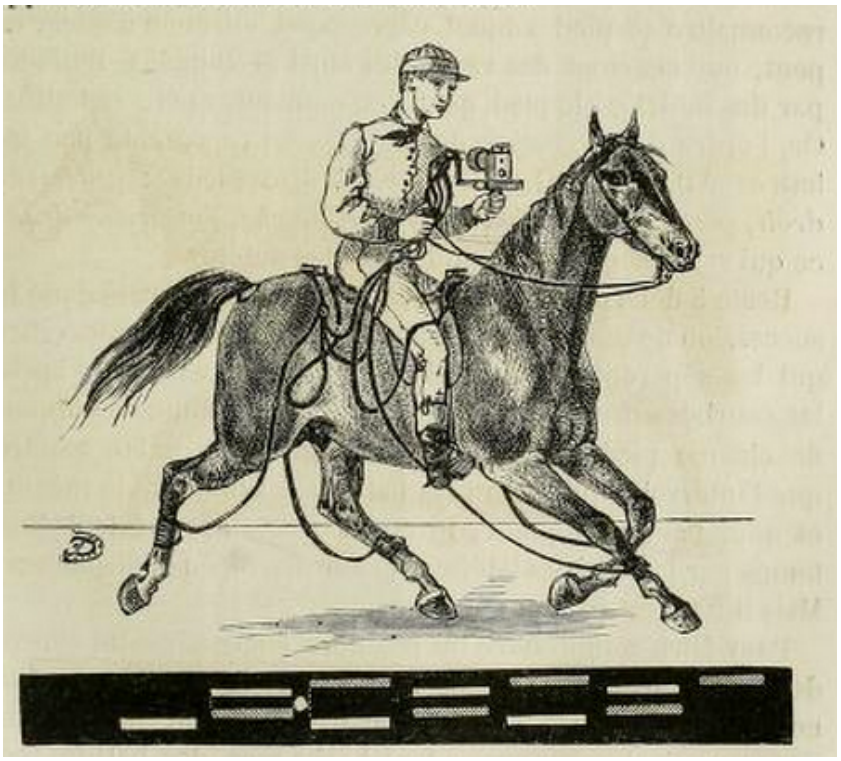

Figure 1.4: An illustration of the contraption Marey built in order to capture the stance-phases of individual legs: a shoe with a small air-chamber was fitted to the horse, with tube connected to a device that measured the change in air-pressure. Synchronizing this with his chronophotographic exposures allowed Marey to accurately categorize different gaits. This illustration is taken from Marey's book *La Machine Animale*, a wonderful digital reproduction of which can be found at the Internet Archive, https://archive.org/details/lamachineanimale00mare.

not handle all aspects of locomotion and limb-coordination[3][33]. How animals solve this seems to largely emerge from a few simple concepts, the most important probably being *decentralized control* in the form of *central pattern generators* (CPGs) and *reflexes*, as well as the *natural dynamics* of the animal. We will go into more detail of these three aspects in a later subsection but first let us how consider locomotion in nature has been approached.

If we consider locomotion as an optimization problem[4], biologists and engineers have inverse problems: an engineer who is designing a robot, for example, knows exactly the cost functions he wants to minimize. The difficult part is understanding the system well enough to actually achieve a solution that both fits the constraints as well as minimizes the cost functions. Biologists observing nature, on the other hand, have direct access to the solution: the morphology, behavior etc. of the animals is already the result of two powerful optimization processes, evolution and learning.

The challenge is then to understand *why* these two optimization processes resulted specifically in this solution, or in other words, what are the cost functions and constraints that form the problem. Of course understanding exactly what the solution is can also pose a challenge, as it is not always obvious how to make specific measurements such as muscle-forces on live animals.

[3]A video of a decerebrate cat on a treadmill can be found on youtube with the keywords "Decerebrate Cat walks and exhibits multiple gait patterns".

[4]Most problems can be formulated as an optimization problem. For legged locomotion we try to minimize things such as step-to-step deviations, stability, energy etc..

1.2.2 Gaits, Scaling and Efficiency

Gaits in legged locomotion can be largely classified by their footfall pattern, as already hinted at by Marey (see 1.1) and more recently expounded on by Hildebrand[19]. These patterns are characterized primarily by 2 factors: the *phase lag* of footfalls, and each foot's *duty factor*. The phase lag determines the order and timing of each foot-fall, while the duty factor of each leg is the ratio of time during which a foot is in *stance phase*, or touching the ground, compared to the overall time of an entire stride-cycle, as such:

$$D_f = \frac{\text{time in stance-phase}}{\text{time of stride-cycle}} \tag{1.1}$$

A duty factor of $D_f = 1$ implies standing or possibly crawling, as the leg never leaves the ground, while in the case of two virtual legs (see subsection 1.2.3), running (i.e. stride cycle including flight-phase) is ensured with a duty factor of $D_f < 0.5$. More generally, a duty factor of $D_f < \frac{1}{\text{number of legs}}$ ensures running, the sum of the stance-phases cannot cover the entire stride, even with no overlap. Note that when the stance-phases of different legs do overlap, it is also possible to achieve running with a duty factor greater than $\frac{1}{\text{number of legs}}$, and the duty factor of each foot need not necessarily be the same as the others.

R.M. Alexander made extensive classifications of these gaits based on the morphology and posture of various animals, with three main posture groups: sprawling, non-cursorial and cursorial as illustrated in 1.5.

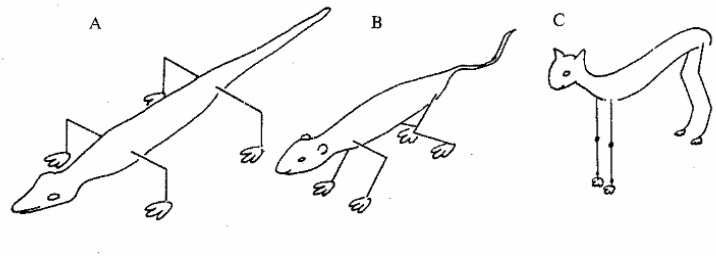

Figure 1.5: An illustration of postures taken from Alexander's paper [2]. The postures depicted in A, B and C are named *sprawling*, *non-cursorial* and *cursorial* respectively. In particular, the evolutionary shift between the bent-knee posture of non-cursorial animals and the straighter legs of cursorial animals has been linked to scaling laws: as volume (and assuming constant density, also mass) scales cubically with size, gravitational forces gain importance very quickly as animals scale up. Consequentially, it generally becomes more important to avoid strongly bent knees which would result in large joint-torques even at rest.

Reptiles generally have a sprawling posture, with legs spread far out from the body. Small mammals and birds tend to be non-cursorial, meaning their legs remain close under the body, but the legs tend to be bent. Cursorial animals encompass larger mammals, with straighter legs.[2]
In order to compare animals with similar posture and morphology but vastly different sizes, Alexander adapted a common engineering concept, the *Froude number*[2][49]. This dimensionless number is commonly used when designing ships and planes in order to compare scaled-down mock models before scaling them up, and is defined as the ratio of the velocity to the characteristic length. For legged animals, this can be redefined in a couple of ways, all equivalent:

$$Fr = \frac{centripetal force}{gravitational force} \tag{1.2}$$

$$= \frac{mv^2/l}{mg} = \frac{v^2}{gl} = \frac{lf^2}{g} \tag{1.3}$$

Where Fr is the Froude number, m and g are mass and gravity, v is the forward velocity, f is the stride frequency and l is defined in different ways, most often as either the leg-length, hip-height at standing, or stride length[49] (the distance between each subsequent step, i.e. the distance covered in a stride). Interestingly, animals of similar posture but very different sizes tend to change gaits at the same Froude number. Hildebrand and Alexander both identified two cost functions that seem to be important in the choice of gaits, namely energy-efficiency and stability. Further studies have suggested that energy-efficiency tends to be more important a cost-function than stability, especially as mass scales up[6].Indeed, if we take a look at the energy efficiency of different gaits at various velocities, the intersections correspond very closely with the velocity at which the animal actually changes gait [47].

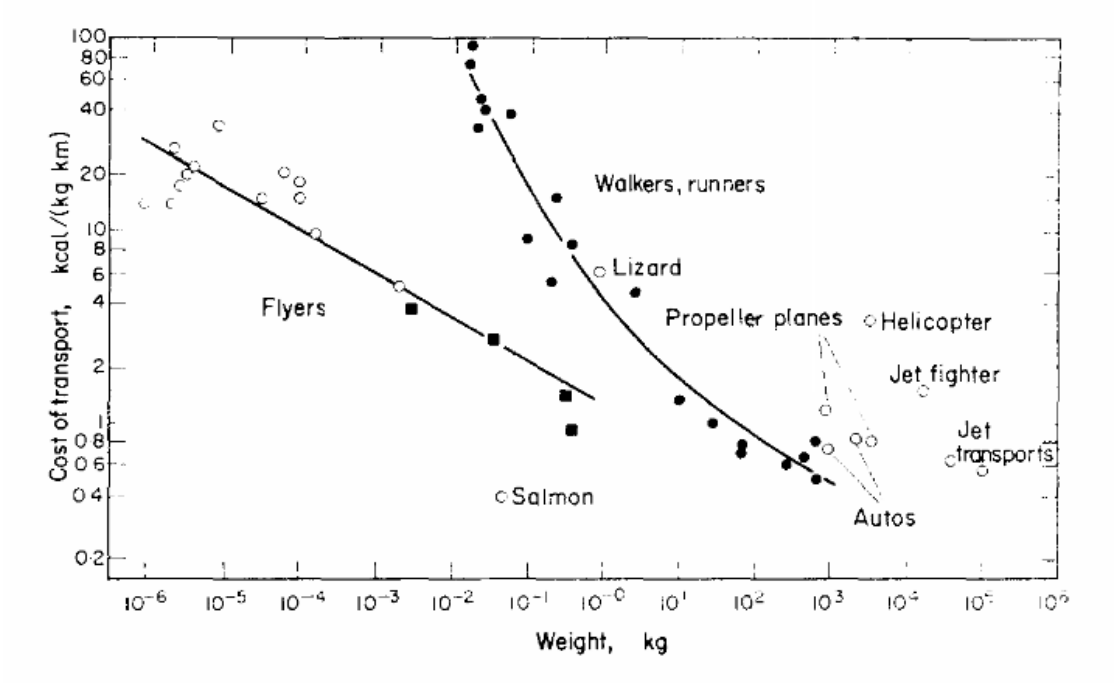

Figure 1.6: Tucker's cost graph shows how the cost of transport tends to scale well with body-mass, although differently for different modes of locomotion.

Again, to better compare animals of different sizes, a dimensionless number was formulated, the so-called *Cost of Transport* or CoT, defined as

$$CoT = \frac{P_{(t)}}{mgv_{(t)}} = \frac{E}{mgd} \tag{1.4}$$

where $P_{(t)}$ is power expended, m and g are mass and gravitational pull, and $v_{(t)}$ is forward velocity. In the second formulation $P_{(t)}$ and $v_{(t)}$ have simply integrated to give E and d, the energy expended and distance traveled, respectively. For many measurements this formulation is simpler as real-time measurements aren't needed. CoT has since become a standard benchmark in comparing the efficiency of robots, especially for comparing them with biological counterparts. However it is important to keep in mind that each gait is an optimal *for a specific posture and specific velocity*! Therefore, especially when comparing with animals, it is important to proceed with caution lest the results be misleading: comparing the cost of transport of a crawling snake with a running human, for most purposes, makes little sense. For some examples of CoT of various animals at various gaits, see [42].

1.2.3 Models, Dynamics and Control

An important step towards understanding the dynamics, and therefore how to control, legged systems is to construct simple models that abstract key components. One of the most successful such models is the *Spring Loaded Inverted Pendulum*, or SLIP model[5], shown in figure 1.7.

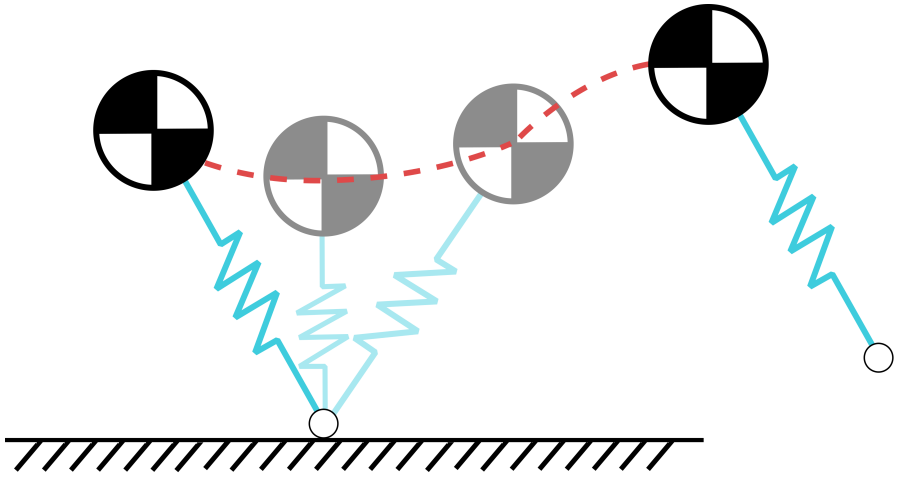

Figure 1.7: The SLIP model represented here in 4 key transition phases: *a*), *b*) and *c*) all take place during stance, and represent foot touch-down, point of maximum spring-compression and foot lift-off respectively. *d*) represents the apex point of ballistic flight.

This model captures the springy action of the muscles and tendons of biological legs, resulting in a smoother transition between a leg's swing and stance phase. This springy action is critical for recycling kinetic energy at impact and therefore allows better energy-efficiency[7][37]. Many studies also show other benefits, for example in increasing the stability of the system[13][15][38] or in decreasing peak forces [4][8][9]. Both for running and walking, the model results in similar *ground reaction forces* (GRF), as those measured experimentally with humans and other animals[32].
This simple model also presents an effective approach for tackling the control problem. Many of the first hopping robots built by Raibert, one of the foremost pioneers of dynamic legged robots, were indeed built in a manner that very closely resembled a SLIP-model, having a single prismatic leg with (springy) pneumatic actuation[40]. The control he devised is split into 3 parts: *hopping height* controlled by adding power during stance, *forward velocity* controlled by choosing the angle-of-attack (AoA) at landing, and finally the attitude of the robot is controlled by hip torque.

Chapter 2

Model and Mathematical Analysis

In order to understand the dynamics of a system it is extremely useful to build simplified, ideal models. By shedding all the details of the real-world system, the complexity can be greatly reduced and it is easier to abstract the most important principles governing the system dynamics one step at a time. Care must be taken that the model isn't over-simplified or possibly important factors are neglected. We build here simple models to understand the effect of a tail on a *qualitative* level, focusing on it's effectiveness as a control-input and how this scales with size.
We keep the definition of a tail as follows:
A tail is a limb that alters the system's dynamics during locomotion without coming into contact with the ground.
Conversely we define legs as limbs that alter the system dynamics primarily through contact with the ground. The importance of this is, while such a limb can induce GRFs during stance it only does so very indirectly: indeed it never directly performs work on the external world, but rather performs work on other parts of the system (body) which then indirectly perform work on the environment. Because of this, such limbs are ill-suited to the control task of adding energy into the system and we hypothesize that this task is taken care of primarily by legs whereas tails, when used for locomotion, are mostly concerned with the task of stability and posture control.
Following this definition, for cases in which the tail exerts appreciable force against the ground we consider it as an additional leg, such as in kangaroo pentapedal gait[27]. We can also consider arms as distinct tails.

2.1 Mathematical Setup

Deriving Equations of Motion

Our models are based on multi-body dynamics with rigid bodies. We derive equations of motion (EoM) with the aid of the second method of Lagrange. I use the notation of C. Glocker[1] and Brian Fabien[12]. These result in EoM of the following form:

$$M_{(q)}\ddot{q} = H_{(q,\dot{q})} + B_{(q)}u_{(t)} \tag{2.1}$$

Where q is the vector of generalized coordinates, $\dot{q}$ and $\ddot{q}$ are the corresponding velocities and accelerations respectively, $M_{(q)}$ is the mass matrix[2], $H_{(q,\dot{q})}$ contains differentiable forces, $B_{(q)}$ is the control matrix and $u_{(t)}$ is the vector of control inputs, all torques or forces. With a careful choice of q, the control matrix $B_{(q)}$ is a constant, linearly independent matrix and can be left out.

[1] C. Glocker held lectures on mechanics at ETH Zurich
[2] We assume in all cases that our systems are fully autonomous, i.e. the mass matrix etc. do not depend on time.

Accounting for Ground Reaction Forces

During stance phase, there are additional contact forces which need to be taken into consideration. In order to maintain the same state vector, we directly solve the GRFs acting on the foot then reproject them into the generalized coordinates.
We have used two approaches for solving GRFs: solving each contact as a linear-complementarity problem with friction and collision-restitution coefficients[16][17], or by making a *no-slip* assumption and then calculating the necessary GRFs to ensure this constraint [41]. While the first approach arguably is more precise it is also computationally more expensive [35] and for qualitative analysis unnecessary.
The interested reader may consult the digital attachments for an implementation of the former method in Matlab. The second method is used both in the simulations implemented in Matlab as well as in the derivations of the dynamics in Mathematica.
Both cases result in an extension of the EoM 2.1:

$$M_{(q)}\ddot{q} = H_{(q,\dot{q})} + B_{(q)}u_{(t)} + J_{c(q)}^{\intercal}\lambda_{GRF} \tag{2.2}$$

where λ_{GRF} is the GRF in cartesian-coordinates and $J_{c(q)}$ is the contact Jacobian of the foot, which we use to project λ_{GRF} into the generalized coordinates.
For the purpose of clarity, it is convenient to rewrite equation 2.2, absorbing the GRF into $H_{(q,\dot{q})}$ and $B_{(q)}u_{(t)}$ as follows:

$$M_{(q)}\ddot{q} = \tilde{H}_{(q,\dot{q})} + \tilde{B}_{(q)}u_{(t)} \tag{2.3}$$

Reformulating as Explicit ODEs

While the algebraic differential equations given in 2.3 are standard and easily solvable with standard algorithms, they are not always easy to interpret. For this reason we directly solve them for *explicit ODEs* as such:

$$\ddot{q} = M_{(q)}^{-1}(H_{(q,\dot{q})} + B_{(q)}u_{(t)} + J_{c(q)}^{\intercal}\lambda_{GRF}) \tag{2.4}$$

$$= M_{(q)}^{-1}(\tilde{H}_{(q,\dot{q})} + \tilde{B}_{(q)}u_{(t)}) \tag{2.5}$$

Again we rewrite this into the standard control form:

$$\ddot{q} = \bar{H}_{(q,\dot{q})} + \bar{B}_{(q)}u_{(t)} \tag{2.6}$$

Where $\bar{B}_{(q)}$ collects all coefficients that multiply a control-input and $\bar{H}_{(q,\dot{q})}$ collects the rest. This allows us to directly examine the effect of each control input on the dynamics of each DoF. Needless to say, the EoM in this form very quickly becomes very large and ponderous to navigate through.

2.2 SLIP Model and Extensions

2.2.1 SLIP Model

We start with the standard *spring-loaded inverted pendulum*, or SLIP-model[5], shown in figure 2.1.
The SLIP model provides a simple approach with rather clear dynamics for running and hopping: during flight phase it is assumed to take on ballistic flight, and the main contribution of the model is to stance-dynamics where the spring-mass pivoting around the foot[3] rather nicely predicts both body-trajectory as well as ground reaction forces (GRFs). The body is modeled as a point-mass

[3]We assume no slipping at the foot

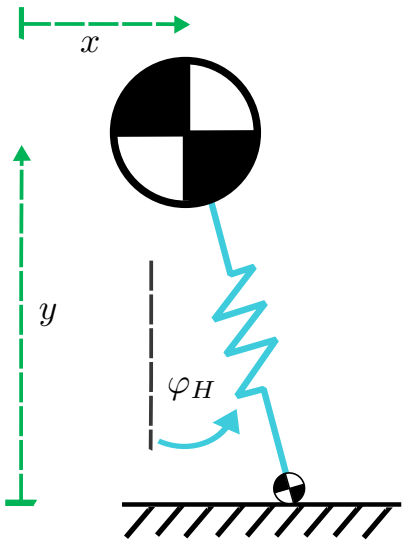

Figure 2.1: The most basic model, based on the SLIP model, has 3 DoFs: horizontal and vertical displacement of body-mass, and hip-rotation. The body mass is modeled as a point-mass without any MoI and hence, without the body-pitch DoF. Note that unlike the actual SLIP model, the hip angle does not automatically reset itself each step but is a continuous DoF. The same goes for the prismatic leg-length, which has been augmented with a foot-mass.

at the hip-joint, with body-pitch and body moment of inertia (MoI) being neglected. Typically control of body-pitch is considered to change only during flight-phase due to torques applied to the leg to reach desired landing angle[4].
When the body's center of gravity (CoG) is at or very close to the hip-joint, this is a very reasonable simplification. However we will show in this chapter that the presence of masses away from the hip joint very quickly complicates the dynamics in significant ways.

2.2.2 Adding Body Pitch

We add body pitch as shown in figure 2.2. Each degree of freedom of a system has an associated inertia: for translational DoFs the associated inertia is a mass, for rotational DoFs it is a MoI. Therefore, to add the pitch DoF, we must also augment the model with the necessary associated inertias.
The implication for the model is that there isn't only a *power-input control task* for maintaining the limit cycle, but also the task of *body-pitch stabilization*. We add body and leg MoI as well as foot mass. Aside from adding to MoI of the leg, the foot mass also adds an *unsprung mass* thus doing away with the energy-conservative nature of the SLIP model. For our purposes it isn't of much importance, however we kept it in the model for completeness.

2.2.3 Adding the Tail

In our second extension, shown in figure 2.3, we add a simple tail as a point-mass connected to the body with a rotational joint via a rigid-body with MoI. It should be noted here that while it is tempting to omit MoI and have only the point-mass on a massless rod, since the added DoF is rotational, its associated inertia is a MoI and not a mass. Indeed in this case if we let the length of the rod l_T go to 0, the presence of the MoI gives it the characteristics of a generic

[4]During stance the hip should be controlled to zero-torque to ensure no destabilizations.

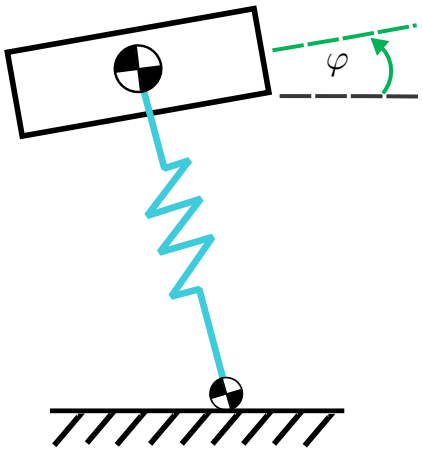

Figure 2.2: We extend the basic SLIP-model with the body-pitch DoF φ, thus adding also the parameter J_S and J_F, the body and leg MoIs respectively, as well as a foot mass. The implication for the model is that there isn't only a power-input control task for maintaining the limit cycle, but also the task of trunk-stabilization. Furthermore, due to the unsprung foot mass, the system is no longer energy-conservative.

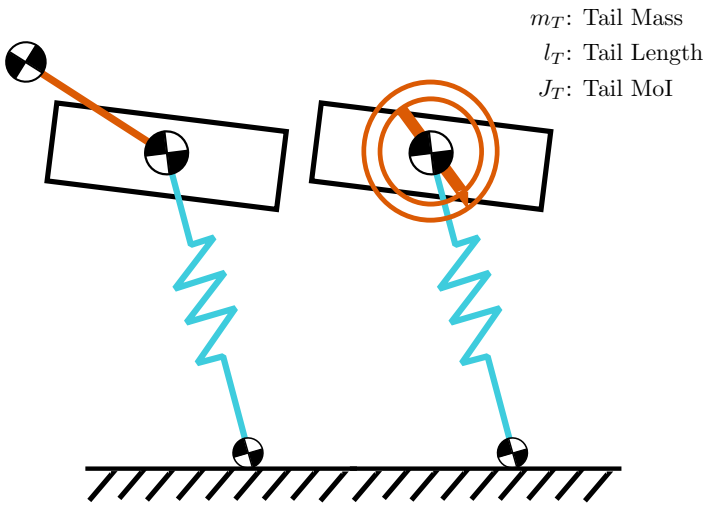

Figure 2.3: We add a tail with parameters m_T, l_T and J_T , the tail mass, length and MoI, respectively. In the representation on the left we let $J_T = 0$ while in representation on the right we let $m_T = l_T = 0$, which is equivalent to a flywheel.

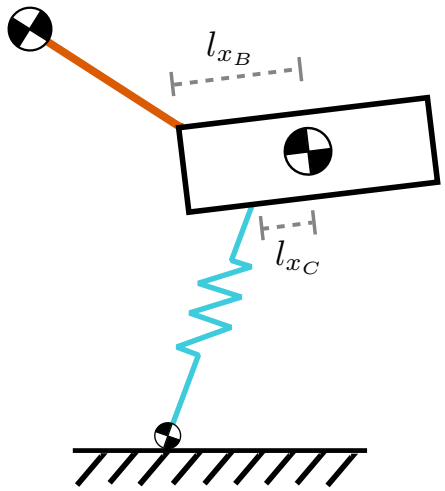

Figure 2.4: In many real-world cases, the body CoG is not centered around a specific joint. This has the effect that in addition to the torques directly actuated at the joint, all forces that bear at the joint also have an effect on the body-CoG displacement and rotations, amplified by the lever-arm, i.e. distances l_{xB} or l_{xC} from each joint to the body CoG.

flywheel. The differences between flywheels and tails will be examined in the next section along with scaling.

2.2.4 Shifting the Hip and Tail Joint

The dynamics from the added pitch DoF are not too complicated when the hip-joint coincides with the CoG of the body: since there is no moment-arm between the joint and the body CoG all torques are transferred very cleanly as torques, and forces as forces. There is no coupling between rotational and translational DoFs. However this changes abruptly when the hip or tail joint is displaced away from the body CoG, as is the case with many animals and robots. This final extension is shown in figure 2.4.
We list all the relevant parameters in the table 2.1. In the previous models some of the parameters are simply set to 0.

2.3 Analyzing Tail as a Control Input

As previously mentioned, our main focus is on the possible use of an active tail in steady-state locomotion. We are interested in the effectiveness of the control input τ_T, the tail torque, on the system dynamics, its possible roles and how this changes with scaling.
While in the simulations we always have springs and dampers at each joint, for the mathematical analysis we discard them. Since we have a control input in the form of a torque/force at each joint parallel to springs and dampers, in our idealized models the resulting torque or force from a spring or damper can be replaced by additional torque from the control inputs: we see that while springs and dampers will make a big difference in the natural dynamics and energetics of the system, they do not alter the effect of the tail and can thus safely be discarded for our purposes.

State Variables	
x	Horizontal displacement of body CoG
y	Vertical displacement of body CoG
φ	Rotation of the body, i.e. pitch
y_F	Prismatic extension of leg
φ_H	Rotation of leg around the hip
φ_T	Rotation of the tail
Parameters	
g	Gravity
m_S	Body mass
J_S	Body MoI
m_F	Foot mass
J_F	Leg MoI
m_T	Tail mass
J_T	Tail MoI
l_T	Tail length
d	Distance from body CoG to hip and tail joints
k_F	Spring coefficient in the DoF y_F
k_{F0}	Spring resting length in the DoF y_F
b_F	Damping coefficient in the DoF y_F
k_H	Spring coefficient in the DoF φ_H
k_{H0}	Spring resting length in the DoF φ_H
b_H	Damping coefficient in the DoF φ_H
k_T	Spring coefficient in the DoF φ_T
k_{T0}	Spring resting length in the DoF φ_T
b_T	Damping coefficient in the DoF φ_T

Table 2.1: Table of state variables and parameters used in the various models.

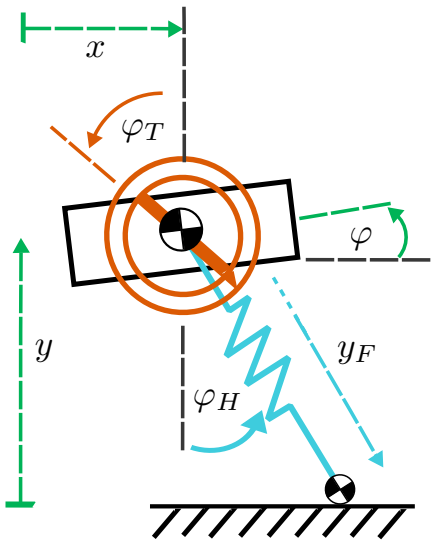

Figure 2.5: Here we depict a SLIP model with 6 DoF: x, y and φ represent the body horizontal and vertical displacements and pitch respectively, y_F represents the leg (or foot) extension, φ_H is the hip angle and φ_T is the angular position of the flywheel (tail). All subsequent models have the same states, simply with modified morphological parameters. Note that in this chapter we have chosen to represent all angles in an absolute reference frame for clarity. For the derivations and simulations found in the digital attachments, φ_H and φ_T are relative to body pitch φ for convenience.

2.3.1 Reference Example: Flywheel with Zero Offset

To build up some intuition for the reader and provide some point of reference, we will introduce briefly the full dynamics of one of the simpler models, a SLIP model with a flywheel instead of tail, where the flywheel joint, hip joint and body CoG all coincide. For reference, see figure 2.5.

For this model, the EoM are as follow:

$$M = \begin{pmatrix} m_F + m_S & 0 & 0 & m_F \sin(\varphi_H) & m_F y_F \cos(\varphi_H) & 0 \\ 0 & m_F + m_S & 0 & m_F \cos(\varphi_H) & -m_F y_F \sin(\varphi_H) & 0 \\ 0 & 0 & J_S & 0 & 0 & 0 \\ m_F \sin(\varphi_H) & m_F \cos(\varphi_H) & 0 & m_F & 0 & 0 \\ m_F y_F \cos(\varphi_H) & -m_F y_F \sin(\varphi_H) & 0 & 0 & m_F y_F^2 + J_F & 0 \\ 0 & 0 & 0 & 0 & 0 & J_T \end{pmatrix} \tag{2.7}$$

$$\tilde{H} = \begin{pmatrix} \frac{g J_F m_S \sin(\varphi_H)\cos(\varphi_H) + m_F y_F \dot{\varphi}_H \sin(\varphi_H)(J_F + m_S y_F^2) - 2\dot{\varphi}_H \cos(\varphi_H)\dot{y}_F (J_F(m_F+m_S) + m_F m_S y_F^2)}{J_F + m_S y_F^2} \\ \frac{g m_S (J_F \cos(2\varphi_H) + J_F + 2 m_S y_F^2) + 4\dot{\varphi_H} \sin(\varphi_H)\dot{y}_F (J_F(m_F+m_S) + m_F m_S y_F^2) + 2 m_F y_F \dot{\varphi}_H^2 \cos(\varphi_H)(J_F + m_S y_F^2)}{J_F + m_S y_F^2} \\ 0 \\ m_F y_F \dot{\varphi}_H^2 \\ \frac{y_F (g J_F m_S \sin(\varphi_H) - 2\dot{\varphi}_H \dot{y}_F (J_F(m_F+m_S) + m_F m_S y_F^2))}{J_F + m_S y_F^2} \end{pmatrix} \tag{2.8}$$

$$\tilde{B} = \begin{pmatrix} -\sin(\varphi_H) & -\frac{m_S y_F \cos(\varphi_H)}{J_F + m_S y_F^2} & 0 \\ -\cos(\varphi_H) & \frac{m_S y_F \sin(\varphi_H)}{J_F + m_S y_F^2} & 0 \\ 0 & -1 & -1 \\ 0 & 0 & 0 \\ 0 & \frac{J_F}{J_F + m_S y_F^2} & 0 \\ 0 & 0 & 1 \end{pmatrix} \tag{2.9}$$

Note that these are the equations of motion during stance, with the GRFs already factored into $\tilde{H}$ and $\tilde{B}$.
For this simple case, the mass matrix M is not overly complex, but still it is not directly obvious how the mixing terms[5] affect the dynamics. We proceed to find the explicit EoM:

[5]The non-diagonal elements of the matrix

Solving these with equation 2.4 leads to:

$$\bar{H} = \begin{pmatrix} \frac{J_F \cos(\varphi_H)(g\sin(\varphi_H) - 2\dot{\varphi}_H \dot{y}_F)}{J_F + m_S y_F^2} \\ \frac{g(J_F \cos 2\varphi_H + J_F + 2m_S y_F^2) + 4J_F \dot{\varphi}_H \sin(\varphi_H)\dot{y}_F}{2(J_F + m_S y_F^2)} \\ 0 \\ y_F \dot{\varphi}_H^2 - g\cos(\varphi_H) \\ \frac{m_S y_F (g\sin(\varphi_H) - 2\dot{\varphi}_H \dot{y}_F)}{J_F + m_S y_F^2} \\ 0 \end{pmatrix} \tag{2.10}$$

$$\bar{B} = \begin{pmatrix} \frac{\sin(\varphi_H)}{m_s} & \frac{y_F \cos(\varphi_H)}{J_F + m_S y_F^2} & 0 \\ -\frac{\cos(\varphi_H)}{m_s} & \frac{y_F \sin(\varphi_H)}{J_F + m_S y_F^2} & 0 \\ 0 & -\frac{1}{J_S} & -\frac{1}{J_S} \\ \frac{1}{m_S} & 0 & 0 \\ 0 & \frac{1}{J_F + m_S y_F^2} & 0 \\ 0 & 0 & \frac{1}{J_T} \end{pmatrix} \tag{2.11}$$

It should now be evident how the explicit ODEs are much more tractable.
Indeed, from equation 2.10 it is can be seen that:

- The DoFs pertaining to each limb (the last three) are exclusively dependent on their respective torque.
- The prismatic leg force y_F only affects the bodies translational DoFs x and y.
- The hip torque τ_H affects all of the body's DoFs, x y and φ.
- The tail torque τ_T only affects body pitch, φ.

For legged-locomotion exploiting natural dynamics we point out that there are two fundamental control tasks, *power input* and *stability*: during steady-state, energy content should remain level, so power must be input into the system to replace energy-losses such as impact and damping. At the same time, the system should not topple and fall, so some control should be expended to keep the system close to it's limit-cycle path. Kinetic energy is contained primarily in the translational DoFs of the body, x and y, and these are the DoFs the power input task is concerned with. The body pitching should integrate to 0 over each stride-sequence, lest the system begin to roll. Keeping body-pitching low is what we mean with the stability task.
In this case, the benefit of the flywheel can be understood by observing $\bar{B}$ in equation 2.10. Both leg-torques τ_F and τ_H can be fully recruited exclusively for the power-input task. The effect of τ_H on body pitching is determined by $\bar{B}_{(3,2)} = -\frac{1}{J_S}$. In the absence of the tail the useful range of the hip-torque in this under-actuated system would be somewhat limited. Instead, this effect can be treated as a simple disturbance, and corrected with the tail-torque τ_T. This is a very powerful consequence: the control tasks of power input for hopping and that of stabilizing body pitch can be cleanly decoupled, greatly simplifying the entire control problem and thus reducing computational load. **We hypothesize that this is a key-advantage for having a tail in locomotion, and that tail design should approximate this SLIP-and-flywheel template in order to decouple these two control-tasks as well as possible.**
Before continuing, we will state what this means as basic design guidelines. We start with an

obvious constraint of the tail. Unlike an industrial flywheel, a tail cannot turn freely forever: it is generally limited to a range of displacement of about π radians. The means that the amount of displacement in body pitch the tail-actuator can cause *per degree of tail displacement* becomes important. This is defined by [24] as *tail effectiveness*, and we reproduce this formula here for the reader's convenience:

$$\varepsilon = \frac{J_T}{J_S} \tag{2.12}$$

where J_S and J_T are the body and tail MoIs, respectively. We see that we can define essentially the same effectiveness ratio directly from $\bar{B}$, and with that make a design-optimization statement:
The tail control input τ_T should affect the body pitch φ by a relevant amount as compared to tail angle φ_T

$$\text{minimize } \alpha_1 \tag{2.13}$$

$$\alpha_1 = \left| \frac{\bar{B}_{(6,3)}}{\bar{B}_{(3,3)}} \right| \tag{2.14}$$

We see here that in this case, this results in the same thing, simply inverted: $\alpha_1 = \frac{J_S}{J_T} = \frac{1}{\varepsilon}$. We do this merely because we state the problem as a minimization, in which case this formulation seems to us more intuitive. During the flight-phase, this equivalence does not change at all. During stance-phase however it can, depending on morphology.
As a second design rule, we state that
The tail control input τ_T should affect the body pitch φ by a relevant amount compared to the leg control inputs τ_F and τ_H.

$$\text{minimize } \frac{1}{\alpha_2} \tag{2.15}$$

$$\alpha_2 = \left| \frac{\bar{B}_{(3,3)}}{\bar{B}_{(3,1)} + \bar{B}_{(3,2)}} \right| \tag{2.16}$$

$$\tag{2.17}$$

If α_2 had a high value, it would take large amounts of tail torque τ_T to neutralize, for example, a small amount of hip torque τ_H. In the case of the SLIP-and-flywheel case, this ratio is a simple $\alpha_2 = 1$. Finally, we state the converse:
The tail control input should *not* affect the body coordinates x and y in a relevant way compared to the effects of leg control inputs.

$$\text{minimize } \alpha_{31} \tag{2.18}$$

$$\text{minimize } \alpha_{32} \tag{2.19}$$

$$\alpha_{31} = \left| \frac{\bar{B}_{(1,3)}}{\bar{B}_{(1,1)} + \bar{B}_{(1,2)}} \right| \tag{2.20}$$

$$\alpha_{32} = \left| \frac{\bar{B}_{(2,3)}}{\bar{B}_{(2,1)} + \bar{B}_{(2,2)}} \right| \tag{2.21}$$

The two ratios measure the ratio of how much the tail-torque affects the x and y DoFs compared to the leg, respectively. Assuming that the body-mass carries most of the total kinetic energy of the system, low values for α_{31} ad α_{32} would mean that the tail has a negligible influence on the power-input control task, but rather that the leg-muscles are more important for this.
For the SLIP-and-flywheel case these ratios are perfectly minimized as the tail-torque has absolutely no influence on x and y.

2.3.2 Basic Tail with Zero Offset

In our second model, we examine a model featuring an actual tail with not only MoI but also length and a point-mass at it's tip, while keeping tail joint, hip joint and body CoG at the same point, as seen in the right model in figure 2.3. The matrices and vectors $\bar{H}$ and $\bar{B}$ are very large for this case and we will not reproduce them here; the interested reader can refer to the digital attachments, where the calculations have been computed symbolically in Mathematica. We examine directly the previously introduced ratios α_1, α_2 and α_{31} and α_{32}.
The ratio α_2 remains the same as before, $\alpha_2 = 1$. This is to be expected as the tail and hip joints remain centered at the body CoG. Thus the tail and hip torque are the only torques that come to bear on this DoF and do so in a clean, direct manner.
The second ratio however no longer disappears:

$$\alpha_1 = \frac{2J_S(m_S + m_T)(J_F + y_F^2(m_S + m_T)}{l_T^2 m_T(J_F(m_T(\cos(2\varphi_H - 2\varphi_T) - 1) - 2m_S) - 2m_S y_F^2(m_S + m_T)} \tag{2.22}$$

Already from equation 2.22, we see that the tail length l_T appears as a second order term in the denominator whereas tail mass m_T appears as a first order term both in the denominator as well as the numerator. This already hints at long, relatively light tails. For the purpose of a simple and clear analysis, we now normalize masses by body mass m_S, lengths by leg-length y_F and MoIs by body MoI J_S. Further, we make an additional assumption, that the leg MoI J_F is negligibly small[6], which results in the following simple equation:

$$\hat{\alpha}_1 = \frac{m_T + 1}{l_T^2 m_T} \tag{2.23}$$

$$= \frac{1}{l_T^2} + \frac{1}{l_T^2 m_T} \tag{2.24}$$

Examining the plot 2.6, we see that indeed having a relatively long tail is more important than having a heavy one, however a certain minimum amount of tail-mass is indeed necessary. Perhaps more surprising however is how quickly the value of α_1 drops in the beginning, and how quickly it pans out. This is quite straightforward once we look at the partial derivatives:

$$\frac{\partial \hat{\alpha}_1}{\partial m_T} = \frac{1}{l_T^2 m_T^2} \tag{2.25}$$

$$\frac{\partial \hat{\alpha}_1}{\partial l_T} = \frac{2}{l_T^3} + \frac{2}{l_T^3 m_T} \tag{2.26}$$

The gradient of α_2 becomes shallow quite quickly, at which point the metabolic cost or other costs of having larger, longer tails probably start to outweigh the benefit.
We examine now α_{31} and α_{32}.

$$\alpha_{31} = -\frac{2(m_T + 1)\sin(\varphi_T)}{l_T(-m_T\cos(\varphi_H - 2\varphi_T) + 2(m_T\sin(\varphi_T)\cos(\varphi_H - \varphi_T) + \sin(\varphi_H)) + (m_T + 2)\cos(\varphi_H))} \tag{2.27}$$

$$\alpha_{32} = -\frac{2(m_T + 1)\cos(\varphi_T)}{l_T(-m_T\cos(\varphi_H - 2\varphi_T) + 2(m_T\sin(\varphi_T)\cos(\varphi_H - \varphi_T) + \sin(\varphi_H)) + (m_T + 2)\cos(\varphi_H))} \tag{2.28}$$

In this case the state of the system, in particular the posture of the tail and hip, greatly affects the coefficients, as can be seen in figure 2.7.

[6] We find the assumption for J_F to match up with most biological as well as robotic legged systems. Considering that the pivot-point during stance is at the foot, the MoI J_F is complemented by $y_F^2 m_S$, which tends to be rather larger. For more convincing, please refer to the Mathematica files in the digital attachments, where values for various values of J_F can be plotted, and indeed they have a small effect on the value of α_1.

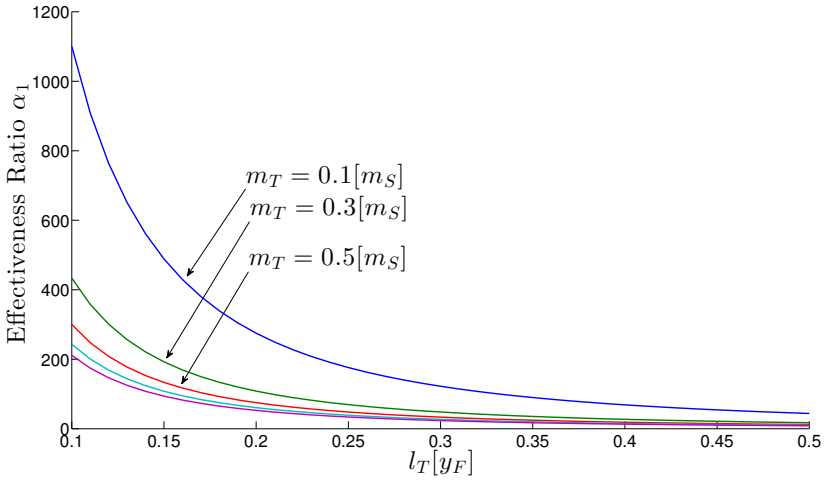

Figure 2.6: The tail Effectiveness ratio α_2 is a measure of how much body-pitch can be countered per degree of tail-rotation. In the figure observe the effects of scaling of the two most important parameters for this ratio: tail mass m_T in terms of the body mass m_S and tail length l_T in terms of leg-length y_F. For the clarity of the graph, we have neglected moment of inertia, as this is determined by the geometry of the tail and can be expressed in terms of m_S and l_T.

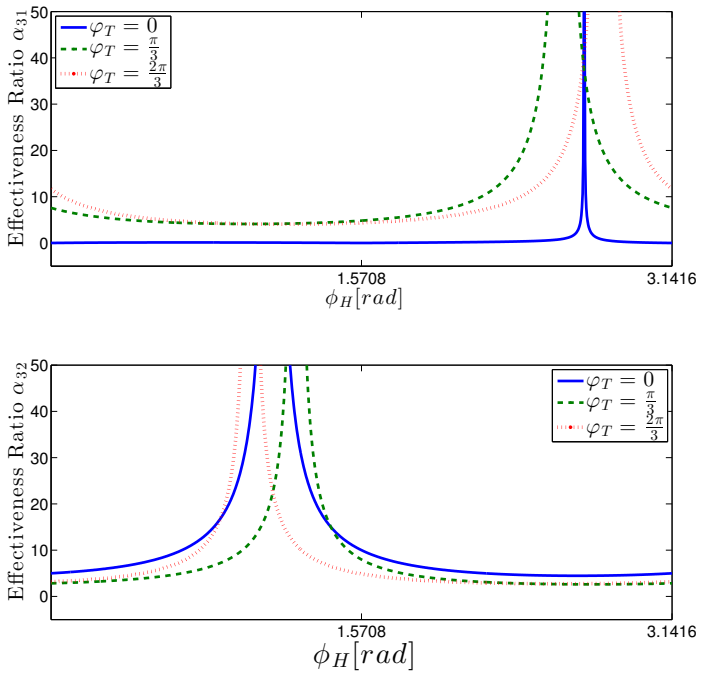

Figure 2.7: The tail effectiveness ratio α_{31} (plotted) and α_{32} measure how much the tail-torque affects horizontal and vertical states of the body x and y compared to leg-torques. In other words, for a low ratio α_{31} the tail is effectively *decoupled* from these DoFs. In the figure we see that for specific combinations of hip and tail angle, a high ratio cannot be avoided. Further, as the coefficients for x and y are perpendicular to each other, these infinities tend not to overlap but jointly cover even more of the state-space.

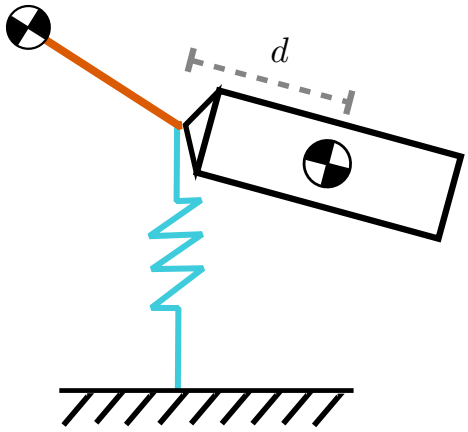

Figure 2.8: We will now look at the effect of having the body CoG off-center with respect to the hip joint. As a simple example we place the tail joint and the hip joint together in order to reduce the number of parameters to a single displacement d. Further, the foot is rigidly fixed the ground with no pivoting, reducing the DoFs by one. In this manner, GRFs can only pass vertically through hip-joint.

When observing the morphological parameters that affect α_{31} and α_{32}, we see that the tail length l_T is present only in the denominator, whereas masses are present in both the denominator as well as the numerator as first-order terms. So again a long, light tail would be the way to go.

2.3.3 Tail and Hip Joint with Offset

In the final example we will examine we shift the hip and tail joints away from the body CoG, as shown in figure 2.4 . This is by far the most complicated model, and the control matrix $\bar{B}$, and hence also the various effectiveness ratios, explode quite quickly and prove very difficult to analyze. The most important effects are however, rather simple to understand intuitively, hence we shall explain them conceptually here, and the reader may consult the digital attachments for a more numerical analysis.

Scaling of Moments of Inertia

We shall approach the case depicted in figure 2.8, where the tail and hip joint still coincide, but are displaced from the body CoG by an displacement d.
The relevant MoIs for the tail actuation is the MoI of tail and body *around the tail joint*, calculated as:

$$J_{tail} = J_T + m_T l_T^2 \tag{2.29}$$
$$J_{body} = J_S + m_S d^2 \tag{2.30}$$

The values of J_{tail} and J_{body} depend on geometry and other factors[7]. Nonetheless, we find that the values are rather well approximated, at least for a qualitative evaluation, as cylinders with

[7]In particular for biological systems, which are not composed of completely rigid bodies, the density of the bodies is also not constant nor do they stay put.

constant homogeneous density. As such, we can simplify the MoIs as

$$J_{tail} = \frac{m_T l_T^2}{3} \tag{2.31}$$

$$J_{body} = \frac{m_S d^2}{3} \tag{2.32}$$

Note that the tail-length l_T denotes not the entire tail length but rather the length from tail-base till tail CoG, comparably to d. The mass is directly proportional to volume, which for a cylinder can be expressed as

$$V = 2\pi r^2 d \tag{2.33}$$

We parameterize the radius r as a function of d, in order to obtain

$$r = ad \tag{2.34}$$

$$V_S = 2\pi(ad)^2 d \tag{2.35}$$

$$= 2\pi a^2 d^3 \tag{2.36}$$

$$m_S = \rho 2\pi a^2 d^3 \tag{2.37}$$

$$= c_S d^3 \tag{2.38}$$

$$\text{with } c_S = \rho 2\pi a^2 \tag{2.39}$$

where a is a constant dependent on geometry, ρ is the body density and c_S is simply a shorthand constant. We use the same procedure to define m_T and plug these results into 2.31 to obtain:

$$J_{tail} = \frac{c_S d^5}{3} \tag{2.40}$$

$$J_{body} = \frac{c_T l_T^5}{3} \tag{2.41}$$

We see that moments of inertia scale very quickly (to the 5TH power), however if scaling isometrically, the tail scales in exactly the same way and can keep up without a problem.

Scaling of Torque-Output

However, we do run into problems when looking at scaling of torque-output requirements. While minimizing the effectiveness ratios α_2, α_{31} and α_{32} to decouple the body-pitch and energy-input control tasks, in order to fulfill the body-pitch stabilization task the tail torque needs to neutralize not only the effects of leg-actuators but also any other forces that cause moments around the body.
We illustrate this with the simple static example of having to neutralize gravitational forces while standing, as illustrated in figure 2.9. In this case, the moment to be neutralized is

$$M_g = \cos(\varphi) d F_g \tag{2.42}$$

$$= \cos(\varphi) d m_S g \tag{2.43}$$

$$= \cos(\varphi) c_S d^4 g \tag{2.44}$$

In the last step we plugged in the previous derivation of body mass from equation 2.34.
From this simple example we see that the moment of gravitational forces scales to the fourth power with size. Not quite as fast as the MoI but still very fast. It is also highly dependent on posture, due to the moment arm $\cos(\varphi)d$

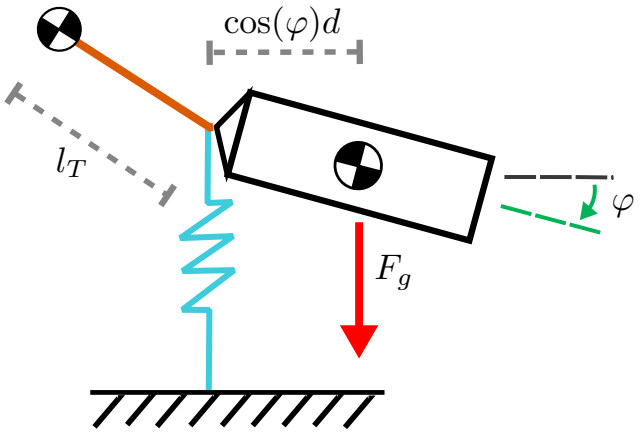

Figure 2.9: As a toy example, we show a standing 1-legged system with a tail. In a static situation, the moment due to gravitational force on the body depends very much on the body pitch angle.

We used a static case to illustrate this effect, however in dynamic locomotion and especially during running or hopping, the GRFs will be the principal force dominating the dynamics. As the impulse during stance needs to match twice the vertical kinetic energy at touch-down in order to reverse the vertical velocity, this force scales directly with mass (impulse is mass times velocity) and therefore cubically with size. The equivalent to the moment arm $\cos(\varphi)d$ in this case would be dependent on the point of attack of the the total combined forces in addition to the posture, as shown in figure 2.10.

the distance between the GRFs and the body CoG. Indeed it has been found that this moment arm is generally kept rather small in most natural-gaits, by controlling the direction of the GRFs to pass very close to the body CoG [1][30].
The redirection of GRFs is of course done primarily through use of the leg actuation, placing some constraints in their use to inject energy into the system. So again, the more the tail is able to counteract these resulting moments, the better it decouples the body-pitch and energy-injection tasks.
Note that the body isn't the only one to be affected by these moments: the tail is of course also affected. Unfortunately, the same parameters that minimize these effects on the tail are the same ones that should be maximized in order to make the tail effective. Careful design can make use of passive elastic elements to counteract a lot of these forces without expending energy, however this tends to make the system efficient for very specific limit-cycles but much less so for others. In other words they tend to lose in versatility.

If these moments are to be counteracted actively, the requirements on the tail-actuators also needs to scale at a similar rate, i.e. to the fourth power with size. However, the force output of the type of fast muscles used in legged locomotion (as well as most man-made actuators) scales roughly proportionately to muscle-mass [28][46], i.e. $\propto d^3$. Assuming that the portion of muscle located in the tail remains constant, the mass of the tail would have to scale at roughly $m_T \propto m_S^{4/3}$ to meet these requirements. This scaling requirement is observed in a similar fashion for leg-muscles[31]. This would not only directly worsen the tail effectiveness, but also increase the moments acting on the tail.

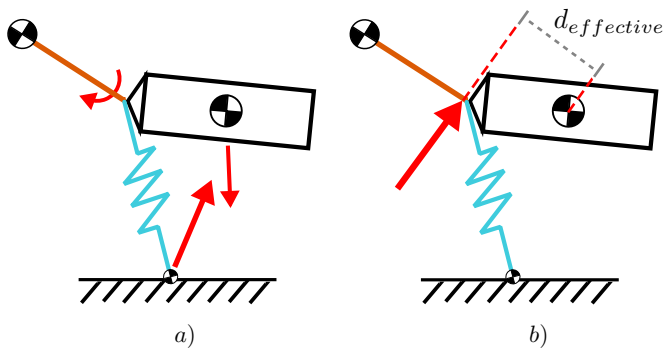

Figure 2.10: During dynamic locomotion, the forces and torques that affect the system are many: it is the perpendicular distance from the body CoG from the resulting force vector that determines the actual effective moment arm. In *a*) we show an toy example with several forces and torques acting on it, and in *b*) the single resulting force and corresponding moment arm. Note that this illustration does not represent any realistic case but is simply used for illustration. Also, the torques are not represented in *b*) simply for clarity.

2.4 Summary and Outlook

Thus we conclude that there are two possible uses for an active tail: one is energy-input into the system, the other for stabilizing body-pitch. For the first, it is necessary to have a strong coupling between tail and body dynamics (in the x and y DoFs), whereas for the second it is only necessary to couple tail with body-pitch (φ) dynamics. We have hypothesized that it is of greater advantage to decouple tail and body dynamics, which leads to a much simpler control problem. We have found that the way to do this is to design a tail that approximates a flywheel, i.e. with a long and light tail.
We have also found that tail MoI is not constrained by scaling, however as animal dimensions scale up, the price in mass for having an effective tail for pitch-control increases proportionally to $\propto d^{\frac{4}{3}}$. From this we expect animals using an active tail for pitch control during steady-state locomotion to be tendentially not too large and/or have a morphology such that the distance d of the body CoG from tail and hip joint be relatively small. Though I have not made an extensive evaluation to see if biological examples fit these results, in many cases they seem to. Amongst the largest animals that utilize in the sagittal plane are kangaroos. Compared to smaller, morphologically similar animals such as wallabies or kangaroo-rats (or smaller species of kangaroos), Grey Kangaroos have very large, thick tails, implying a geometry which favors higher mass for the same tail-length.
Snow leopards are another large animal which appear to actively use their tails for pitch-control: again the tail is much larger than other similar cats which don't use the tail. Further, snow leopards are most often observed to use the tail while hunting mountain goats on near-vertical cliffs, downwards. In such a situation, the apparent moment arm $\cos(\varphi)d$ would indeed very

small, again explaining why they are able to make effective use of the tail while other similarly sized animals don't.

Chapter 3

Simulation

We have simulated the models developed in chapter 2, synthesizing open-loop control inputs while optimizing cost functions in order to evaluate optimal solutions. Note that in most cases the solution space is highly non-linear and we do not look into any guarantees of achieving global optima. We will however refer to solutions as "optimal" as short-hand, meaning that we have made extensive effort to improving them. We have performed these optimizations on the idealized models presented in the previous chapter (as well as some others, for details see digital attachments) in order to evaluate the *qualitative* implications of the additional tail-torque control input on optimal steady-state locomotion. By numerically finding optimal control inputs for different parameter configurations as well as different cost-weighting, we can numerically evaluate the usefulness of the tail. We will start by first introducing the tools we've used for simulation, then proceed to the discussion.

3.1 Tools

3.1.1 Simulation Framework

I initially developed a framework in Matlab for simulation which worked based on time-stepping algorithms and impact-models [16][17], however we then primarily used the Matlab framework for legged-locomotion developed by C. Remy [41]. This second framework use hybrid-dynamics without solving the linear complementarity problem at impact, making it slightly less accurate; also it makes the assumption of no-slip at contact points. For qualitative analysis, we found this to be more than sufficient, not to mention that the solving times were decidedly faster. Since most of the modeling concepts in both frameworks were very similar[1], the derivations could be quickly ported over. Also other members of the BioRob lab had some experience with Remy's framework already and it also provided an already-implemented graphical visualizer as well as tools for control-input synthesis and analysis.

Open-loop Control Input

For synthesizing open-loop control trajectories, we implement a direct torque or force source[2] at each joint. Parallel to these we add springs and dampers. Since the torques and forces produced by the springs and dampers can be arbitrarily replaced by their parallel actuators, the reachable state-space is not altered by their presence unless the actuators have bounded. Springs and dampers do however make it easier for the optimization algorithms to solve, as the natural dynamics will already tend towards a limit-cycle. Further, they strongly influence the optimal

[1] Both are based on Lagrange's second method, see chapter 2

[2] For brevity we will henceforth use the term torque interchangeably for torques and forces, and simply intend forces when it refers to a prismatic joint, and torque for rotational ones.

control inputs when optimizing with cost functions.
For finding a control trajectory for each torque-source we simply define them as a truncated *time-based Fourier series*:

$$\tau_{(t)} = a_0 + \sum_{n=1}^{N} a_n \sin(2n\pi f_{stride} t) + b_n \cos(2n\pi f_{stride} t) \tag{3.1}$$

Where $\tau_{(t)}$ is a time-dependent torque trajectory, a and b are the fourier coefficients, t is time and f_{stride} is the stride frequency. In our idealized simulation we are searching for limit-cycle locomotion without any disturbances and therefore expect a periodic control trajectory. With a sufficient number of Fourier coefficients, an arbitrary smooth control trajectory can be rather well approximated. One drawback of this method is that each coefficient influences the shape over an entire stride-cycle, instead of the control-input at a specific time of the stride-phase. Because of this the number of coefficients to be optimized can be kept low, however we cannot create truly arbitrary trajectories. More importantly, this approach somewhat limits the directions of the gradients in which the optimization can proceed: increasing the amplitude at a specific point implies also changing it everywhere else. Other control functions have been tested, however not extensively used. Their main drawback is the curse of dimensionality. For details, please consult the digital attachments.

Synthesis Tools

The framework includes two tools for finding periodic solutions: FindPeriodicSolution and FindPeriodicSolutionDIRCOL. Both make use of the gradient-based solvers fsolve() for finding periodic solutions and fmincon() for optimal periodic solutions, both standard from the MATLAB Optimization Toolbox. By setting specific terminating event such as flight-phase apex, foot touch-down or foot lift-off, the synthesis tool treats the difference in intial-states and terminating states as constraints, i.e.

$$\mathbf{x_{INITIAL}} - \mathbf{x_{TERMINAL}} = 0$$
$$\mathbf{x_{INITIAL}} - F_{(\mathbf{x_{INITIAL}})} = 0$$

where $\mathbf{x_{INITIAL}}$ is a vector containing all continuous and discrete states that we want to make periodic at initial conditions, $\mathbf{x_{TERMINAL}}$ is the same vector at the terminating condition, and $F_{()}$ represents the executed simulation of the hybrid-dynamic system until the terminating condition, and is therefore $F_{(\mathbf{x_{INITIAL}})} = \mathbf{x_{TERMINAL}}$.
The second tool, FindPeriodicSolutionDIRCOL, implements direct-collocation[45] which greatly speeds up convergence. The price is that events must be predetermined for the algorithm: while this is trivial for a monoped system, for a multi-legged system the exploration path may not stray from the initially defined footfall pattern.
While the present synthesis tools are very useful, they present an important drawback: since both tools are gradient-based, having an initial guess that is already within the basin of attraction is critical. For many of our models (in particular, once the hip-joint is moved substantially away from the body CoG) finding a good initial guess is extremely tricky: even manually found solutions which would hop for several steps and looked to be intuitively very close to stable were often not good enough for the algorithms to converge. Thus, to make these tools more versatile, we've implemented the following modifications:

1. Toggle to use the MATLAB Global Optimization Toolbox to search for global minima. While this essentially solves the problem of requiring a good initial guess, it is generally extremely slow. Especially when using relatively high order Fourier-series for the control inputs, the number of starting points explodes very quickly.

2. Possibility to redefine periodicity constraints as a regular cost function. This "relaxes" the constraints and treats them as regular cost functions to be minimized. This is useful when the direction of the optimization gradient violates the constraints of specific states.

3. Possibility to define specific target terminating values instead of periodicity. This was used during attempts to split a stride-cycle into different parts and optimizing each individual part. This approach was not explored thoroughly.

While these have helped in some cases, they tend to require quite some tinkering as well. A simpler more rapid approach was used: the particle swarm optimization framework developed at the BioRob lab.

3.1.2 Particle Swarm Optimization Framework

The BioRob Lab disposes of a Particle Swarm Optimization (PSO) framework running on a cluster[48][11], which allows for relatively fast searches for global minimas without requiring a deep understanding of the cost functions and dynamics of the system to be optimized. For the models we use, this is extremely useful as the dynamics are of high order, highly non-linear and with non-smooth impacts (i.e. hybrid dynamics). For the aforementioned gradient-based synthesis tools it is therefore critical to supply a good initial guess. Despite great efforts to find a semi-automatic method of obtaining initial guesses, I was not successful as small changes in model parameters had a great influence on the dynamics. With the PSO framework, it is however possible to find a good initial guess with a very simple and generic cost function: *maximise distance travelled in a specific time, while constraining maximum control input.* By restricting the maximum control input we avoid a situation where one giant leap is taken. Though some tinkering is still needed, with a long-enough horizon, the solutions found by the PSO often tend towards periodic gaits. Evaluating the fitness of these population already provides a lot of insight into the problem, in particular regarding the importance of different parameters. More importantly, we obtained solutions that were close enough to steady-state that we could then use the gradient-based solvers to find true stable local-optimums.

3.2 Control Results from Local Optimization

With the previously described local optimization tools (see subsection 3.1.1), we can observe how the presence of a tail influences the reachable optimums under different conditions and different cost functions. For this purpose, we use quasi-periodic solutions found via the PSO optimization process and then apply the local solvers on them. We apply two steps here: first a periodic solution is found without optimizing a cost function. This result is then used as the initial guess for finding optimal solutions that minimize a specific cost function while at the same time retaining the same constraints. We present here the most relevant results, starting with the SLIP-and-flywheel model (see chapter 2) and then proceeding to more complex models.

3.2.1 Cost Functions

For our optimizations we maintain the assumption that most animal gaits, especially steady-state gaits, are chosen for being energy-efficient [47]. As such, the cost functions we use are to minimize energy expenditure. There are different ways of doing this. Here, instead of minimizing energy input to the system, we choose to minimize energy losses, i.e. damping and impact losses. Since periodicity of the limit cycle is enforced as a constraint, all energy-losses must be replaced through positive work. Though we do not directly model the internal dynamics of the actuators, we do keep track of their associated losses by modeling them as idealized electro-motors and track their losses due to internal resistance. Thus we define three sources of energy loss, two in the mechanical domain and one in the electrical. The mechanical losses are defined as:

$$\text{Impact Losses: } E_I = m_F \dot{r}^2_{F(TD)} \tag{3.2}$$

$$\text{Damping Losses: } E_D = \int P_d dt = \int b_x \dot{x} dt \tag{3.3}$$

where m_F is the unsprung-mass of the foot (which is our only contact point) and $\dot{r}_{F(TD)}$ is the velocity of the foot at touch-down, P_d is power-loss through damping, b_x is a damping coefficient attached to the x joint[3] and $\dot{x}$ is the velocity of the associated joint. In the electrical domain it is essentially the same:

$$\text{Electrical Resistance: } E_R = \int P_r dt = \int R_x I_x^2 dt \tag{3.4}$$

$$\text{with } I = \frac{\tau_x}{K_x} \tag{3.5}$$

where R_x is the internal resistance of the motor of that DoF, and I_x is the current passing through that motor. We further assume no gearing[4], and thus can find I_x through it's directly proportional relation with the motor torque τ_x via it's motor constant K_x.
As we usually use touch-down as the initial (and terminal) condition during the optimization, we can often leave out impact losses as they cannot be influenced by the control inputs without violating the periodicity constraints.
For most optimizations we also assume that the majority of energy losses come from energy losses in the motor, and thus mostly modify the internal resistances R of the actuators rather than modifying the mechanical damping in the joints. This gives us more freedom to use the mechanical damping coefficients to help find stable gaits.
It should be noted that while these electrical losses are modeled after electro-motors; biological actuators, i.e. muscles, have different losses. These are not explored here.

3.2.2 Cost of Transport

Cost of Transport (CoT) is an often used benchmark to compare animals as well as recently bio-inspired robots[47]. It is defined as:

$$CoT = \frac{W_{tot}}{mdg} \tag{3.6}$$

where W_{tot} is the total mechanical work performed or energy expended for locomotion, m is the mass displaced, d is the distance displaced and g is gravitational pull. In our simulations, we keep track of total work performed by actuators, setting

$$\dot{W}_x = P_x = |\tau_x \dot{x}| \tag{3.7}$$

where $\dot{W}_x = P_x$ is the power expenditure around the specific joint x, this being equal to the force or torque applied times the velocity, $\tau_x \dot{x}$. We keep track of the absolute value of this, as the sign simply indicates whether the actuator is performing positive or negative work. In both cases, it is energy expended.
We will frequently use CoT as a benchmark to compare different optimization runs with different cost functions and/or paramters.

3.2.3 SLIP-and-flywheel

For our first step we use the simplest model, the SLIP-and-flywheel introduced in the previous chapter, see 2.3.1, as a proof of concept and test that under different conditions a tail (or in this case flywheel) can indeed improve performance by allowing all leg actuators to be used exclusively for power-input. As shown in 2.3.1, with a pure flywheel instead of tail, and with both flywheel-joint and hip-joint placed directly at the body CoG, the flywheel-torque only affects the flywheel

[3] We use x as an arbitrary joint and DoF, it has no reference to the DoF x in the models we've used.
[4] Gears are a common source of energy-losses in real systems.

itself and body pitch: it has absolutely no effect on forward or upward acceleration, and therefore cannot be used to change the momentum. Therefore it lends itself well for a proof of concept.

We start by running optimizations with 4 different conditions and cost functions:

Free-spinning Flywheel The states of the flywheel are not constrained to be periodic, creating a more realistic flywheel. The cost of both leg-actuators are equal.

Periodic Flywheel The states of the flywheel are constrained to be periodic, as a tail would be. The cost of both leg-actuators are equal.

Hip torque penalty The hip torque τ_H is penalized at a 50:1 ratio in the cost function, making it very expensive. We expect the majority of power input to be performed by the prismatic leg-force τ_F, and stabilization to be provided by the flywheel.

Prismatic Leg-force penalty The leg force τ_F is penalized at a 50:1 ratio in the cost function, rendering it very expensive. We expect the majority of power input to be performed by the hip-torque τ_H. Since this destabilizes body-pitch, we also expect the flywheel-torque τ_T to increase considerably in order to counteract the hip torque.

We show the results of the most interesting parameters in the two following figures: body pitch φ, hip angle φ_H and tail angle φ_T along with CoT in figure 3.1, and the required torques in figure 3.2.
As expected, the last case with a heavy penalty on τ_F has a much higher CoT of 8.6730, on entire order of magnitude higher than the cases where hip and prismatic-leg torques are penalized equally. From figure 3.2 we also see, as expected, that the recruitment flywheel-torque τ_T is strongly linked to that of hip-torque τ_H, and is also much much greater in the final case. What is somewhat surprising is that in the first case, where the states of the flywheel are not constrained to remain periodic, they in any case do not deviate.

3.2.4 SLIP-and-tail

We shall now look at a more relevant case for understanding tails: a SLIP-model with tail-joint coinciding with the hip-joint and body CoG, as shown in section 2.2.3. We have run various optimizations, always by first finding good initial guesses via the PSO optimization in the cluster and then running gradient-based optimizations to find an actual local-minima. The results fit with the prediction made in the previous chapter that a long-light tail should be more effective and allow for more effective actuation.
As a showcase we compare two hoppers: both have tails with identical MoI, and thus α_1 (see chapter 2) is the same for both cases, however in the first this is achieved with a short but heavy tail, whereas in the second with a light but long tail. The resulting optimal control-inputs are shown in figure 3.3.
The lighter tail does indeed result in a lower cost of transport. Observing the graphs, we also note that the hopper with the lighter tail keeps it's control inputs much closer to 0 compared to the one with the heavy tail. This makes sense with the concept of a decoupled-control, as whatever actuation the leg produced during stance would be easier to counteract during flight by the tail, and could then more easily be reduced to 0. Since during flight-phase we have purely ballistic-flight and no energy can be injected into the system, controlling the robot to the proper landing state should be the only control task. For a decoupled-system, it should be relatively easy to quickly arrive at a proper state then simply continue to "free-fall" without any additional actuator-input, and hence no more cost.
We remind the reader here that, as explained in the subsection 3.1.1, we do not perform a

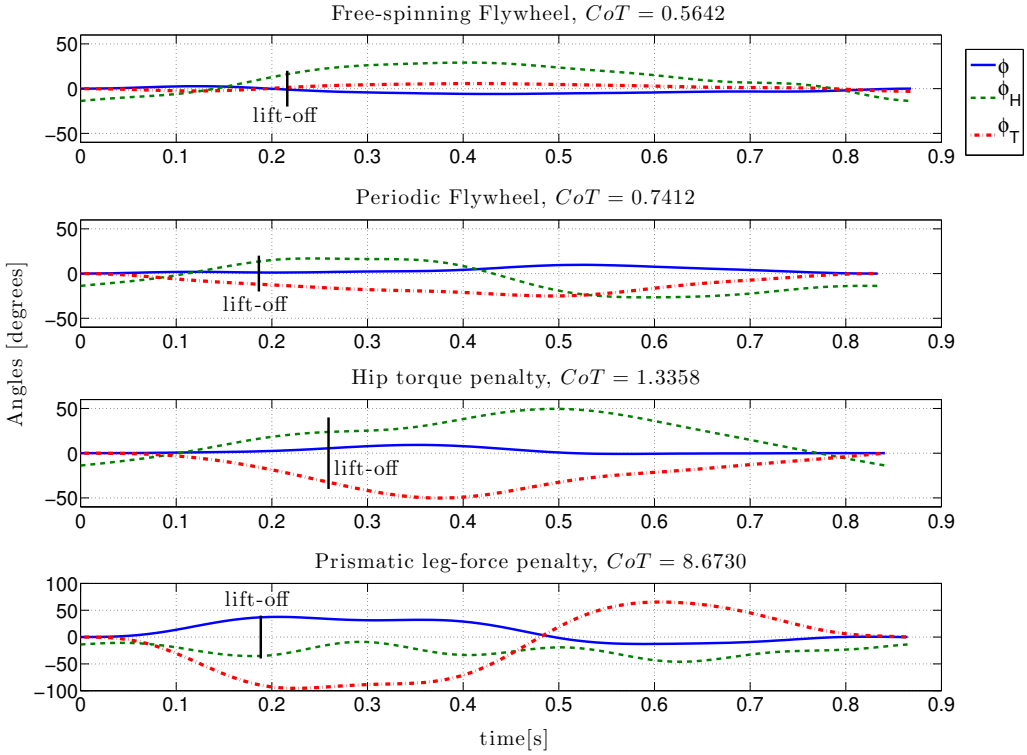

Figure 3.1: We evaluate the body-pitch φ, hip-angle φ_H and tail-angle φ_T of the SLIP-and-flywheel model, optimized with 4 different cost-functions. The graphs show an entire stride-cycle, starting and ending with foot touch-down. The point of lift-off for each case is marked with a vertical line. In the first, the costs are all held equal, but the states of the flywheel are not constrained. In the second, we add periodicity constraint to the flywheel states. In the third, the hip-torque is strongly penalized. In the fourth, prismatic leg actuation is strongly penalized. Note that y-axis in the last plot has a different scaling, as all states fluctuate more.

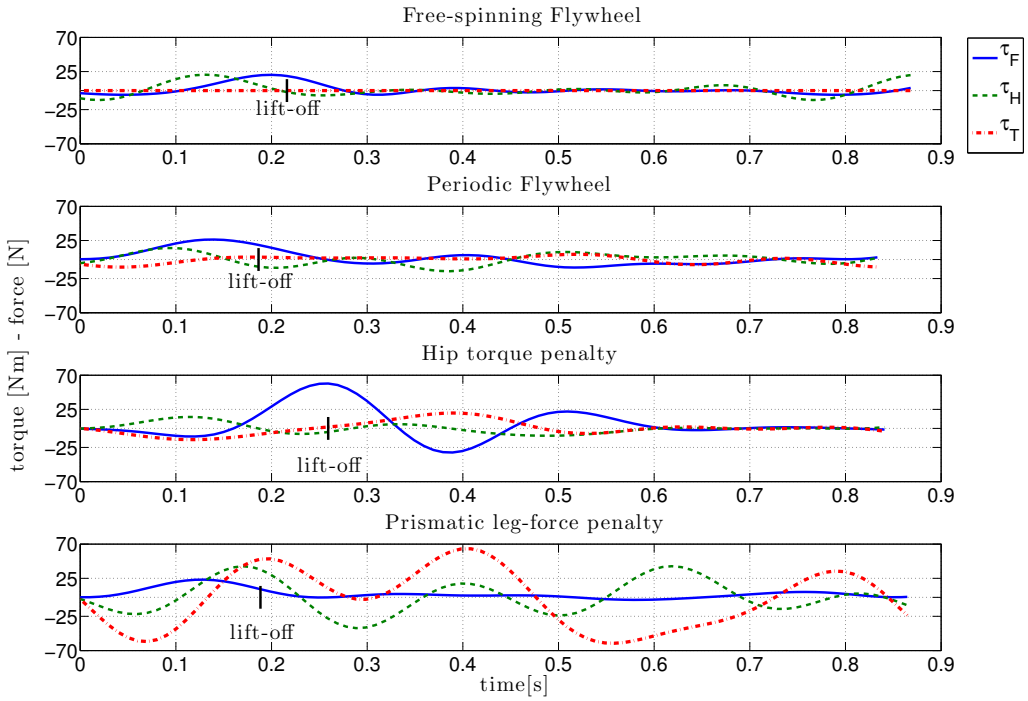

Figure 3.2: Here we show the torques and forces of the three actuators in the same four optimized models described in figure 3.1. As one would expect, in the fourth the hip provides a much larger portion of power. As a result, the flywheel needs to also work a lot more in order to neutralize the disturbances of the hip-torque on body-pitch. Note also that the lesser the constraints, the quicker the control inputs go to 0 after lift-off. Since during the flight-phase we basically have ballistic flight, actuator input is only necessary for reaching the proper configuration, or posture, for landing. Control inputs should therefore be minimal.

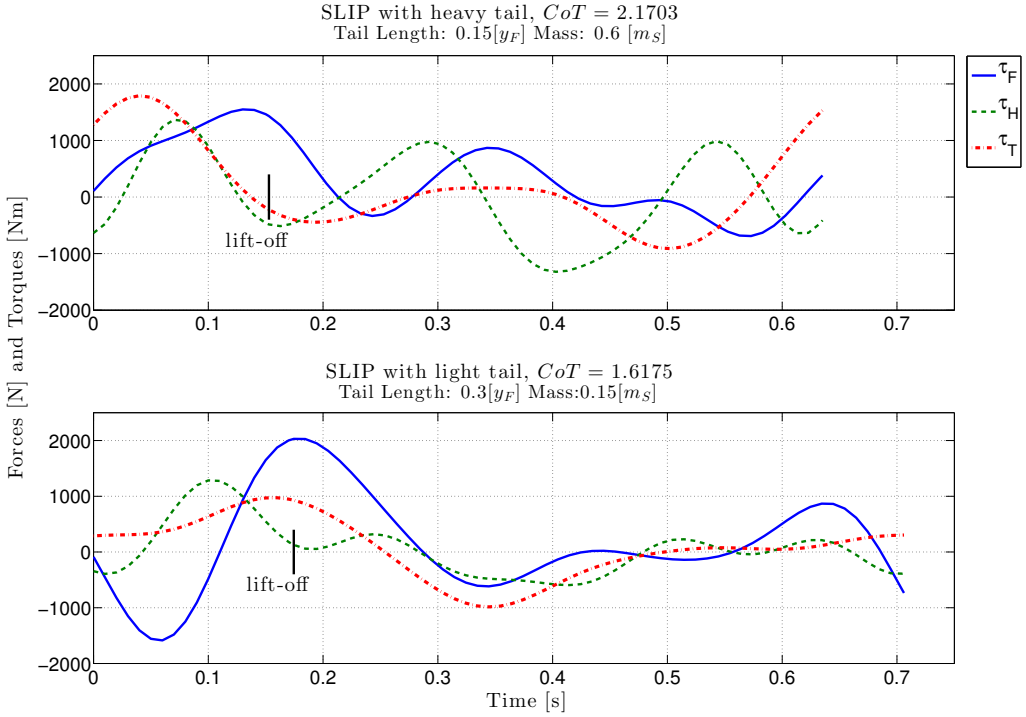

Figure 3.3: As an example, we have two cases of SLIP-model hoppers with a tail. Both tails have the same MoI, however one is short and heavy whereas the other is long and light. The long and light one clearly expends less effort during flight-phase, and it also manages to achieve a lower cost of transport. The MoI of both tails are calculated assuming a cylindrical structre, with $MoI = \frac{ml^2}{3}$, m being mass and l being length.

completely free trajectory optimization. Since we base the control input on a truncated Fourier-series, generally truncated at 5 coefficients, we can achieve a rich, but not a completely arbitrary trajectory. Also not all trajectories can be reached via gradient-descent from an arbitrary point.

3.3 Summary and Outlook

We have numerically optimized both morphology and open-loop control trajectories for monoped-hoppers, comparing tails with different parameters. For the optimization, a combination of PSO algorithms and gardient-based algorithms have been used in order to search a wide parameter-space for a global optimum, then use that as a starting point to find the local optimum. The simulation and optimization results presented match the predictions made in chapter 2: optimizations with a longer, lighter tail perform better in stabilizing pitch. At the same time, better CoT was found in for the lighter tail as well. While this doesn't go against any of the predictions, we feel that this may simply be an artifact of the optimization procedure: we have shown in chapter 2 that shorter, heavier tails have stronger coupling between tail and body dynamics. Though we haven't discussed this mathematically, from experience we know that the basin of attraction for limit-cycles often becomes narrower and more specific for highly-coupled dynamics. In other words, the system is less forgiving, in terms of energetic cost, for not hitting the actual resonance frequency. This again actually matches with the predictions: a stronger coupling could potentially be more efficient but sacrifices in terms of controllability and versatility.
Stability analysis was started, however not thoroughly completed at the time of writing. The approach taken is to use Floquet-analysis to generate a first-order linearization of the return-map, and then use the control Jacobian of the return map to modulate the control trajectory, in an effort to close the loop and stabilize the system. In preliminary results, the closed-loop models never do worse than their open-loop counterparts, and in some cases manage to take several more hops before falling over. In particular, we compared stability against body-pitch perturbation for the two example-models shown in 3.2.4. The long, light tailed model indeed was able to take several hops more compared to it's open-loop reference, whereas the model with the short, heavy tail showed no improvement. We find that these preliminary results are promising and warrant a more thorough stability analysis, including finding a completely stable closed-loop form, is recommended. To this end, a new asymmetric leg design should be considered, in an effort to increase the passive stability properties[18][32]. This would allow focus to be put on on body-pitch control and efficient energy-input, without having to care so much about stabilizing the gait itself.
Also, during the thesis we have focused above all on the use of the tail for body-pitch stabilization, however further investigation on actually increasing coupling in order to increase efficiency could also be rewarding, particularly for engineering applications. Indeed, human-made machines are very often designed for very specific tasks, in which case sacrificing versatility in favor of efficiency could be the better option.
Finally, a quadruped model was also implemented (see digital attachments) but not extensively test. A major advantage of the monopod is it's simplicity: not only does it have much fewer parameters to tune and analyze, it also displays essentially one gait: hopping[5]. Nonetheless, investigating the tail use with different gaits can also be very interesting. Indeed, in the hardware tests presented in the next chapter, chapter 4, we specifically used the bounding gait as the normal trotting gait of the robot displayed virtually no body-pitching, making the tail superfluous for pitch-control in that gait.

[5]Numerically, other gaits can be found, such as pirouetting, however these can be quite immediately discarded.

Chapter 4

Hardware Experiments with Cheetah-Cub

We used the Cheetah-Cub robot [44] to explore the use of a tail also in hardware. Cheetah-Cub is a simple and small quadruped with two actuated DoFs per leg, hip and knee-flexion, roughly the size of a house-cat and lighter at 1 kg (house-cats generally weigh between 3 and 5 kg). The Cheetah-Cub features very compliant pantographic legs which make it robust to impacts, and more importantly allow for very stable and fast *open-loop* locomotion: feed-forward position-control inputs are fed directly to the servo-motors, generated from a simple CPG network. Stability is provided by the mechanical morphology of the robot and indeed for the trotting gait there is an extremely wide set of parameters for the CPG which remain completely stable. This allows the CPG to be tuned for performance, i.e. forward speed, without worrying about stability issues. The robot has achieved an impressive velocity of 6.9 body lengths per second, and is capable of step-downs of over 10% hip-height with over 80% success rate[44].

For the experiments we designed and built a 1-DoF rigid tail fitted to the Cheetah-Cub in the sagittal plane and subsequently also built an improved version of the cheetah-cub as well as a second tail which we mounted at the front of the robot and used as an actuated neck and head. For all aspects of the hardware development I am very much indebted to François Longchamp and Daniel Chapuis. François is a technician at BioRob who took care of virtually all the manufacturing and was also very helpful for assembling as well as coming up with ideas for how to best implement certain design aspects. Daniel is an intern with a background in watch-design, who took care of the CAD drawings for me and with whom I had several brain-storming sessions on how to design individual components as well as the entire assembly. Figure 4.1 shows the CAD design of Cheetah-Cub with tail, and figure 4.2 shows a real Cheetah-Cub robot with two tail-modules mounted: one at the back acting as a tail and one at the front acting as a neck and head.
We used this robot to explore in hardware the function of the tail in generating steady-state gaits, focusing on the bounding gait. Analysis has been done using high-speed video and motion capture technology. Measurement of ground-reaction forces was used however no meaningful conclusions were taken from them, and they will not be presented here.

4.1 Hardware

4.1.1 Tail Design

For the tail design we wanted the following features:

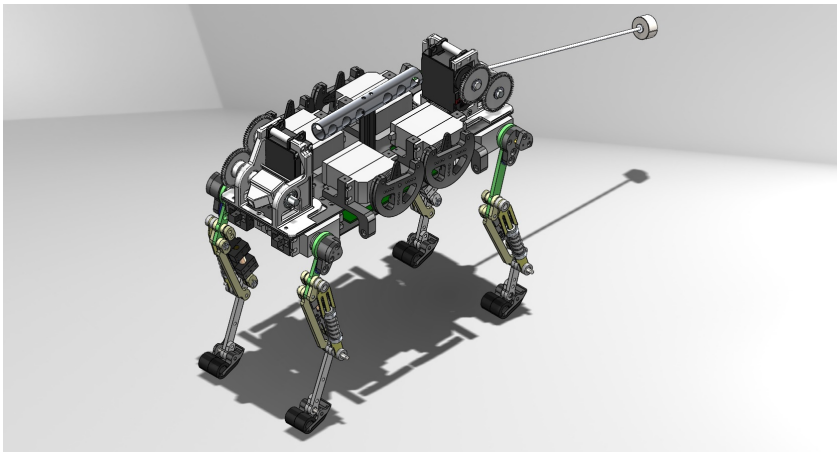

Figure 4.1: A CAD rendering of the Cheetah-Cub with the tail mounted.

Light-weight so that the tail structure does not drastically influence the overall dynamics.

Modular design such that the design-parameters tail length, mass and MoI can be quickly and easily adjusted.

Simple and Robust as a small and light robot, the Cheetah-Cub often falls and tips over, but is also very robust to impacts. The tail should also have these properties, as it makes testing much more viable.

The final design of the tail-base can be seen in figure 4.3.
The main tail-base is the only 3D-printed part of the tail structure and incorporates the mounting for the motor and tail-axle. We have iterated the design once, increasing support around the tail-axle and simplifying the support structure for the motor, as well as increasing the surface of the surface area used to mount the tail-base to the body-base. The contour of the tail-base has been designed to fit snugly with the body-base and knee-motor support structure, so that forces generated by the tail are transmitted cleanly to the main body without excessive torsion.

A simple transmission with 1:1 gears couples the motor to the tail-axle, allowing the motor to be placed directly behind the main base and centered in the coronal plane. Since the motor represents the largest mass of the tail-system, having it centered is important for not destabilizing the system. We chose to use the same motors as the Cheetah-Cub: Kondo KRS-2350HV ICV Reds. This meant we could use a lot of material already present on hand, also we can directly control the motors from the RB-110 RoBoard of the Cheetah-Cub, making synchronization of tail and legs a cinch.
Two ball-bearings ensure minimal friction at the tail-joint even at high speeds and accelerations. A connecting element made out of POM plastic is fixed to the tail-axle, with a brass female M3 screw tapped fit into it. This allows tail fitted with a threaded end to be screwed into place or removed very easily and quickly.
The unassembled parts of the tail, as well as fully assembled tails can be seen in figure 4.4. The main support structure of the tail is a hollow carbon fibre tube. On one end a steel screw-in base is attached with two-component epoxy glue: this allows the tail to be quickly screwed on and off of the tail-base mounted on the robot. We switched to a steel screw-in base on the tail as the aluminum ones used in initial trials sometimes bent out of shape due to the large moments applied by the tail.
On the other end, a threaded aluminum rod is fixed with two-component glue. This threaded rod is used to easily adjust the weighting of the tail. Brass weights of different mass can be easily

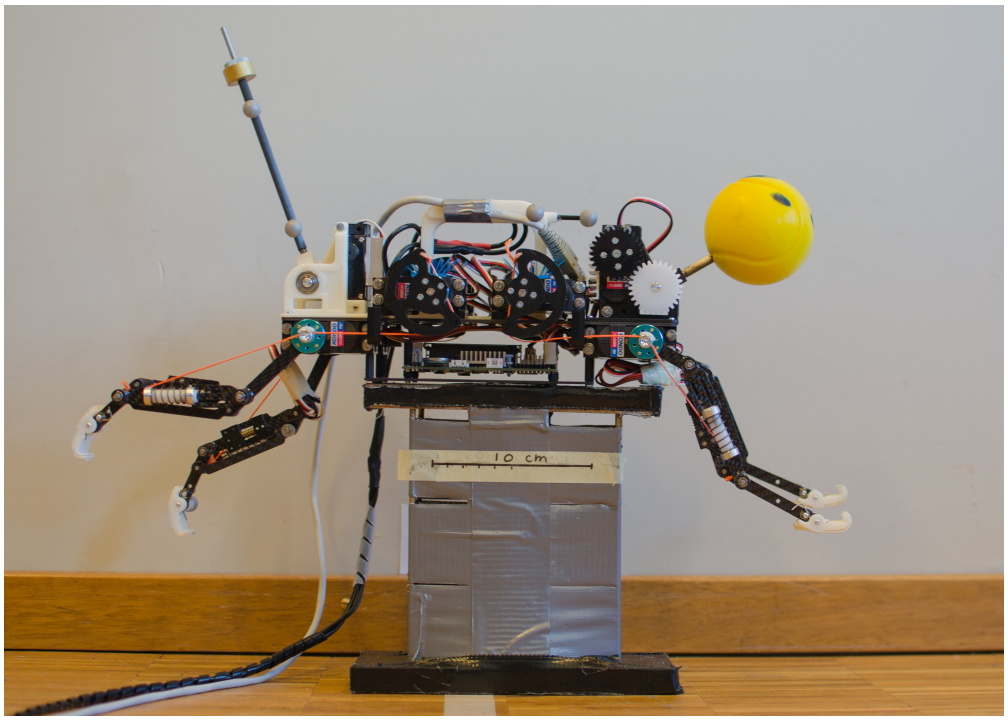

Figure 4.2: The fully assembled Cheetah-Cub, including a foam-head. Note the reference-scale taped on stand, 10 [cm].

slipped onto this bar and held in place with aluminum nuts. Each nut weighs an additional 5 grams, making them also very useful for fine-tuning the weight.
Since the carbon fibre tubes are extremely light-weight and stiff, these tails can be well approximated as rigid-bodies with a point-mass at the tip and low MoI. For measuring the MoI of a tail, we find it's CoG by balancing it on a thin edge, and calculate the MoI around the tail axle via parallel-axis theorem.

4.1.2 Updated Cheetah-Cub

We built a new version of the Cheetah-Cub, internally affectionately dubbed CheetahCub Blue. This version is conceptually the same as the old Cheetah-Cub, but resolves issues of wear and tear on the old robot[1] as well as various small improvements in design and ease of use. François gets credit for the bulk of the redesign as well as impeccable high-precision manufacturing. The improvements are briefly listed here.

Improved Leg Design with the knee flexion cable shifted to be centered much closer to the joints. This greatly reduces the lateral torque exerted on the legs during knee flexion, which can cause leg-deformation in the long run.

Precision Manufacturing particularly for the legs, minimizing friction in the joints as well as the differences in dynamics between legs. In the old Cheetah Cubs, the springiness and friction of each leg sometimes varied from leg to leg, which often caused instability.

Heat-Sinks have been placed on the motors to improve thermal disspation. Especially when using the motors at more than 9V, they tend to overheat very rapidly, severely limiting

[1] The old Cheetah-Cub has been used in countless experiments for over three years by now.

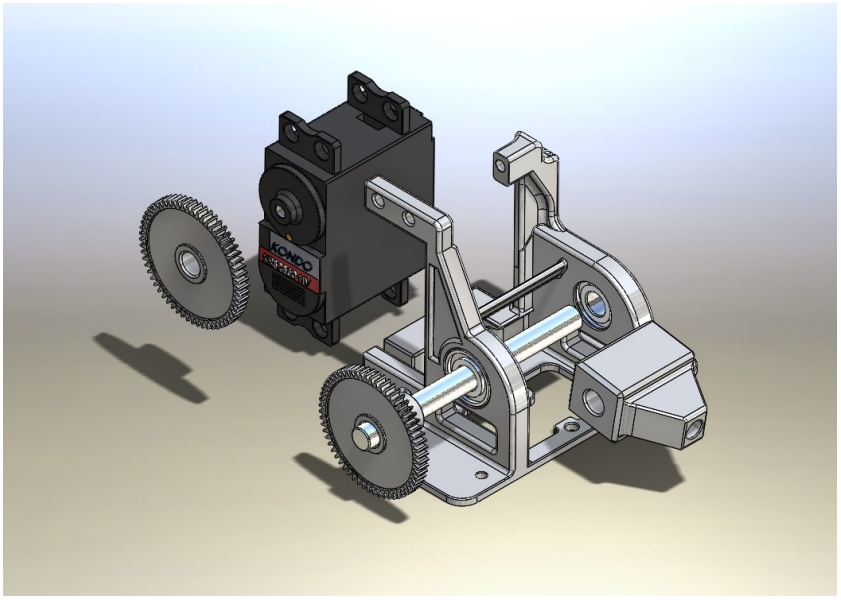

Figure 4.3: A CAD rendering of the tail-base, without the mounted tail. A transmission with 1:1 gearing allows the motor to be placed compactly directly behind the tail-axle. Since the motor is the heaviest component of the tail-base, centering it is important so as not to destabilize the robot.

the continuous testing time. This despite the fact that the motors are rated 9V-12V[2]. In the history of the Cheetah-Cubs many motors have been burnt out in this manner.

Simplified Assembly use of only standard pieces and consistent choice in screw-types etc., making repairs much simpler.

Improved Handle which directly attaches to the body base-plate, providing a more even transfer of forces than the previous handle, which was mounted to the life-side motors, causing minor torsion. Further, mounting points for motion-capture markers are integrated in the handle eliminating the need for a separate structure. Finally, special hinges have been added to secure both the power cables as well as an ethernet cable. Unreliable connections (both in power and communication) have been a recurrent nuisance during experimentation. The hinges ensure that any tugs on the cable are transferred through the handle and directly to the robot body, without putting any strain on the cable connectors.

4.1.3 Control and cȯdγn

On the Cheetah-Cub a RoBoard RB-110 running a custom Xenomai RT-linux takes care of all computation. For more details see [44]. To simulate the CPG and generate outputs to the motors, we use cȯdγn[3], a high-level mathematical language to elegantly describe coupled dynamics. This language allows easy generation of extensive CPGs, easy adjustment of the couplings between them, as well as quick and easy tuning of parameters during experimentation. We connect to the robot via ssh, allowing direct access to all parameters in real-time.

[2]See http://kondo-robot.com/product/krs-2350hv-ics-red-version
[3]See chapter two of [25] or www.codyn.net

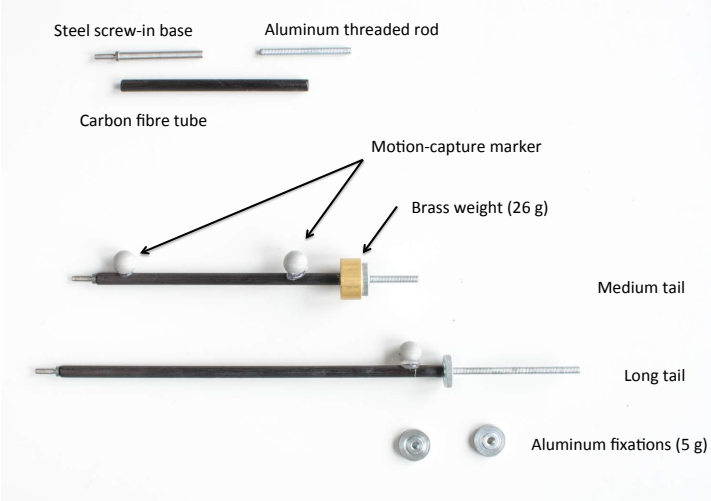

Figure 4.4: At the top the unassembled components of a tail are shown, as well as two finished tails and the manners of adjusting the tail weights.

4.2 Exploring Tail Function with Bounding Gaits

For exploring tail function we chose to focus on the *bounding gait* instead of the trotting gait, which has been the focus of experiments with the Cheetah-Cub so far. In the bounding gait the front pair of legs and hind pair of legs move in unison, as can be seen in figure 4.5. In the trotting gait, because of the positioning of the stance-legs, the total GRFs during each stance-phase tend to pass very close to the body CoG, causing little to no changes in angular momentum. Indeed, unless the control parameters of the CPG are very poorly tuned, the robot exhibits virtually no pitching during steady-state trotting. Further, the two stance-phases in a single stride-cycle are virtually symmetrical.
This is in stark contrast with bounding: because the GRFs are generated either by the hind- or the fore-legs, in each case the entire orientation of the body compared to the leg-pair in stance is completely different. We saw in chapter 2 how this can be very important.
Since the tail motor directly acts on the pitch DoF and pitch-control is what we expect the tail to be most useful for, we wanted a gait that is asymmetrical in the sagittal plane, where body-pitching is not only present but actually an important part of gait-generation.

4.2.1 CPG Network with Tail Node

In figure 4.6, the structure of the CPG network including tail-node, is shown. For the exact description of the dynamics of nodes and edges of the network, we refer to [44]; here we briefly give a quick overview of the parameters important for understanding our results.
The CPG network we use two different types of nodes: the hips and tail use a regular sinusoid-based *phase nodes*, whereas knee flexion nodes have special *double-peak nodes* (for more details see [44]). The knee nodes only have monodirectional edges from their respective hip node and therefore directly phase-lock with these. The hip and tail nodes instead are all connected to each other via bidirectional edges. For bounding, we fix the edges between left and right hips at 0 phase-lag i.e. they move together, and omit them in our representation for clarity.
Regarding phase-lag between tail and legs, we are usually interested in the phase-lag between the tail and the hind-hips and thus generally remove the edges between the fore-hips and the

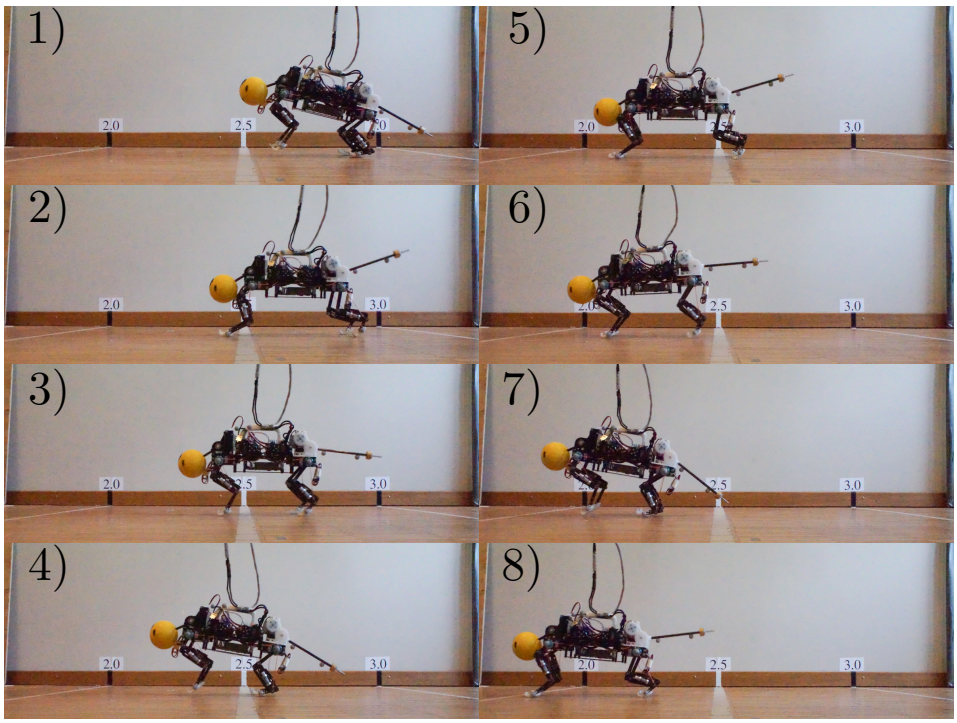

Figure 4.5: A typical sequence of bounding with the Cheetah-Cub.

tail node by setting the coupling weight to 0. Note that the same phase lag could be achieved without adjusting the coupling weight, but it is much less intuitive to do. In table 4.2.1 we highlight the most relevant parameters of the CPG network and of the phase nodes.

Network Parameters	
f	Frequency
ξ_{hf}	Phase-lag hind to fore hips
ξ_{ht}	Phase-lag hind hips to tail
Phase Node Parameters	
O	Offset
A	Amplitude
D_f	Duty Ratio

4.2.2 Parameter Search for Bounding Gaits

We conducted an extensive search of the parameters to find not only a well-performing set of parameters, but also to analyze which parameters were important and what their effect is. We conducted this parameter search in different configurations: without the tail, as well as with tails with different configurations. We present here the most relevant conclusions. We also refer

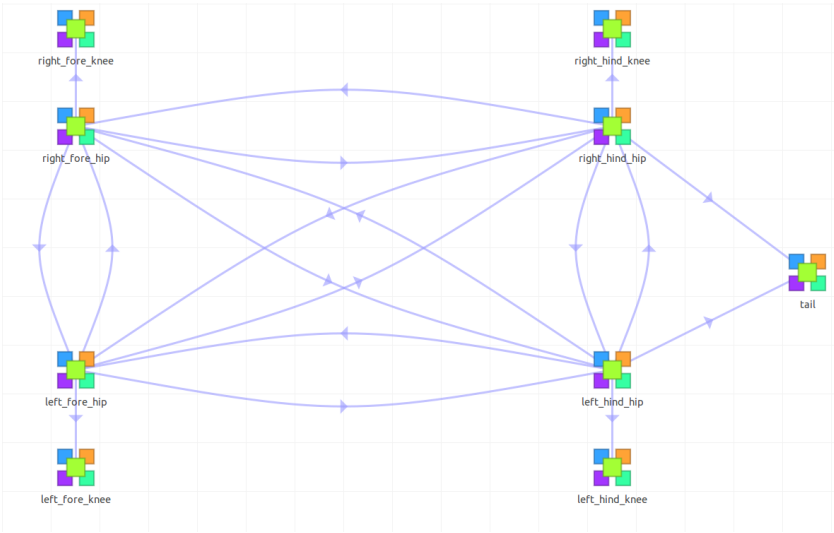

Figure 4.6: The CPG network, generated with codyn. Each node represents one motor, and it's output is a position control signal that is sent to the servo-motor. The edges represent the coupled-dynamics, i.e. which nodes affect which others. For clarity, only the edges between the hind-hips and tail are shown while those from the fore-hips and tail are omitted. Also, no neck-node is shown, though this is perfectly symmetrical to the tail node.

to the digital attachments, which include high-speed video of many runs.
For recording data we use a motion capture system, with markers placed on the robot, the robot's legs and the tail. We have also recorded GRFs using force-plates, however no relevant conclusions were deduced from it and we do not show them here.

Bounding Without a Tail: Hind-Foot Placement

Bounding without a tail presented a rather interesting case. The single most important parameter to tune was the hind-hip offset O_h, which determined the AoA of the hind-feet at touch-down. If this was not perfectly tuned, Cheetah-Cub's feet would either slip on the floor without performing any useful work on the body and "run on the spot", or it would actually bound reasonably quickly, but backwards. With the aid of high-speed video recordings, we determined that the importance of the hind-leg placement was to be able to properly load the hind-leg springs; without compressing the hind-leg springs, insufficient vertical GRFs are generated during the rest of the stance-phase to provide the necessary traction for the motion of the hip-motors to perform positive work. It should be noted here that the knee-flexion is a uni-lateral DoF: the motor can only retract the leg, while extension is performed passively by the springs in the legs. This means that when the knee-cable is taut, extension-power is limited on the one hand by the force of the spring and on the other by the extension velocity of the knee-motor: the knee-motor absorbs a lot of the extension power through the cable. Hence, to generate power in the *axial* DoF it is necessary for the springs to be loaded while the knee-cable is slack.
We show in figure 4.7 a tuned bounding gait without tail.

Bounding With a Tail: Hind-Hip to Tail Phase Lag

In bounding with a tail, we first found parameters for a reasonable bounding gait, i.e. hip-offsets and amplitudes, knee flexion etc., then explored the effect of the tail parameters:

- offset

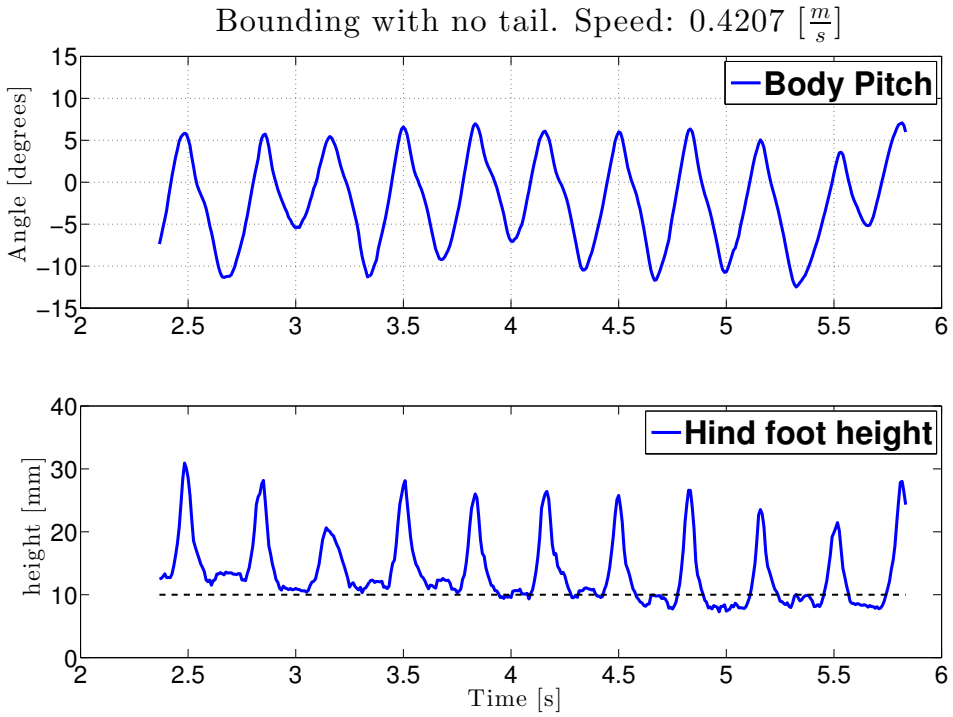

Figure 4.7: During steady-state bounding without a tail, the body pitches roughly 15 degrees per stride. In the second plot the height of the hind foot is shown, to give an idea of the hind-stance phase for reference.

- amplitude
- phase-lag

The most important of these has been phase-lag: adjusting the phase-lag often led to faster, but more importantly to more stable and smoother gaits. Adjusting the offset had an effect only when making large changes, where the tail went from parallel to the ground to being perpendicular to it. As a perpendicular position was rarely very effective, we have performed most explorations with the tail offset parallel to the ground. We have tested tails with various parameters, each time performing a rudimentary parameter search along the most important CPG-parameters to find a good gait. We show here two reference examples. In figure 4.8, we used a long and light tail (which can be seen in figure 4.4). With the tail we were able to achieve a marked improvement in forward speed and the robot was less prone to tipping and falling on it's side. We attribute to a more regular gait with less body-pitching. Indeed the body-pitching is also reduced, from roughly 15 degrees per stride to roughly 10, and it's phase compared to the hind-stance phase is much more regular.
In figure 4.9, we use a shorter but heavier tail. Note that the total MoI around the tail axle is the same as in the run shown in figure 4.8. Again, we see the same improvement over the tail-less robot with regards to body-pitching. We also were able to find a higher forward speed again. By observing the high-speed videos (see digital attachment), we determined this to be caused primarily by reduced slipping of the hind-feet. The slipping was thereafter captured using the motion capture system: the trajectory of one of the hind-feet in the x and y plane for the three presented runs can be seen in figure 4.10.
The reduced slipping is probably due to the added inertia produced by the tail at the end of it's down-swing, which in turn causes greater GRFs and therefore better traction. This would

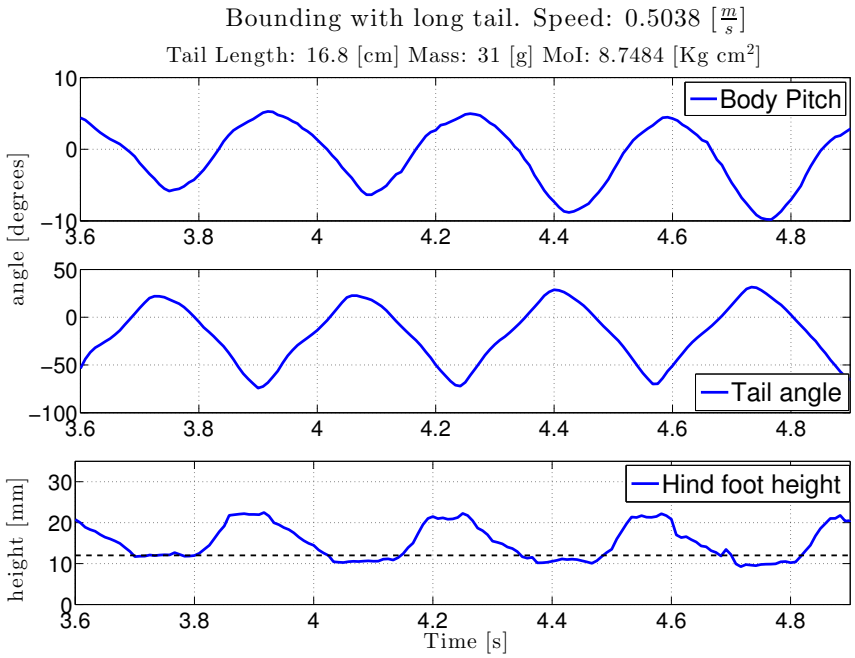

Figure 4.8: In this run a long and light tail was used. Note the increase in speed as well as the reduced body-pitching.

also explain the reduced performance when the tail offset is set perpendicular to the ground. In comparing this with our simulated model, we see that the no-slip assumption does not hold. In our hardware tests, slipping is a critical factor and source of wasted energy, and because of this there is a great benefit from actually coupling and coordinating the control of leg and tail. In short, though the tail has reduced the burden on the leg-actuators of stabilizing body-pitch, completely decoupling the controls is not necessarily the optimal solution in this situation.

4.3 Summary and Outlook

We have designed and implemented a simple 1 DoF tail for the Cheetah-Cub robot and tuned CPG-parameters to achieve the bounding gait. Analyzing performance, we have identified the most important CPG-parameters for bounding, as well as evaluated the effect of having no tail or a tail with different morphological parameters, i.e. mass and length. The results have shown that a tail does indeed improve body-pitch stabilization, and that a heavy tail, i.e. with strong coupling (see chapter 2), can improve performance by injecting energy into the system.
More complex tails, possibly with compliance or more DoFs, present an interesting follow up. Also, sensorizing the Cheetah-Cub robot with feet-contact sensors and an IMU or simple gyroscopes would allow for closed-loop control, which would be an ideal addition.

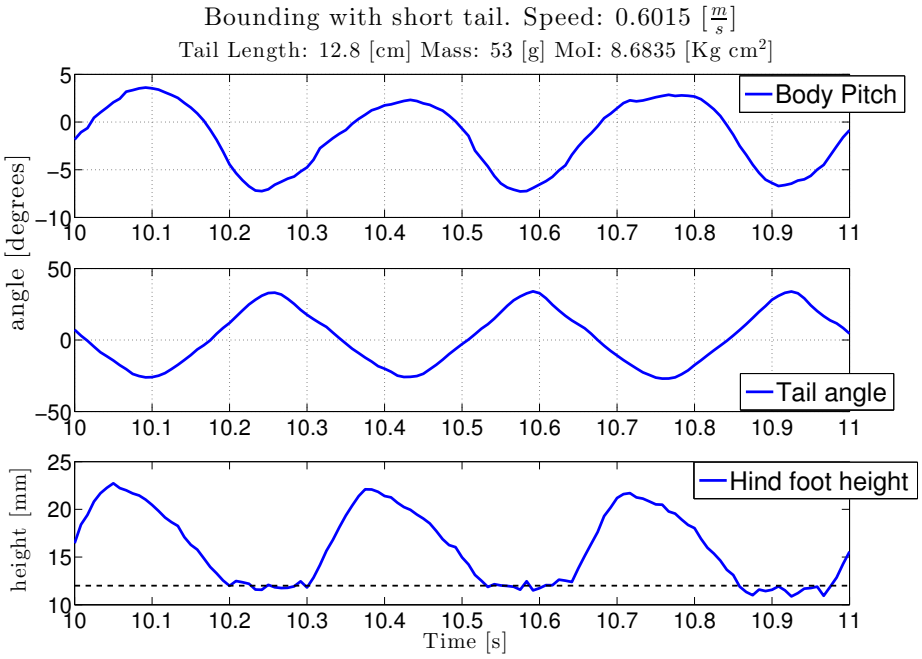

Figure 4.9: In this run a shorter, heavier tail was used. Note that the total MoI around the tail-axle is very close to the longer, lighter tail. Though the amount of body-pitching is similar, we were able to attain a markedly higher forward speed.

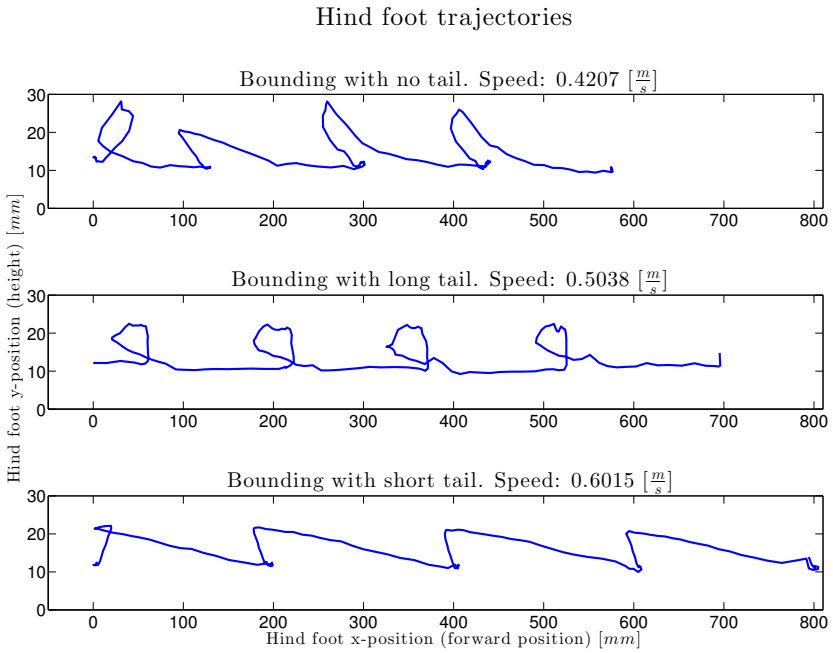

Figure 4.10: The trajectories of the hind-foot in all three cases (no tail, long and light tail, short and heavy tail) are shown here. For the parameter values of the tails, please see figures 4.8 and 4.9 respectively. From the trajectories, it can be seen that without the tail foot placement and traction is very irregular, and during the forward swing the foot actually slides along the ground. With the long tail the foot still slides along the ground, however the pattern is already much more consistent from step to step. With the shorter but heavier tail, the foot moves backwards very little during a stride, and during the swing-phase cleanly clears the grounds. In this last case, a greater portion of the stride is used to perform positive work on the body, and there is also less negative work through friction overall. We represent the hind-foot as the tail-node in the CPG network is coupled with the hind-hips, and it's effect is most pronounced and visible on the hind-feet.

Chapter 5

Conclusion

5.1 Summary of Tools and Results

In chapter 2 we have presented a series of simple models, starting from a SLIP-model[5] and step-by-step adding additional components, from flywheel to tail to a tail with tail-joint and hip-joint displacement. This allows us to more easily analyze the effect on the dynamics of each component. In the ideal case, a SLIP-and-flywheel, we find that two important control tasks for locomotion, body-pitch stabilization and energy-input, can be effectively decoupled and thus simplify the control problem. We hypothesize that this is a key advantage of an active tail, and thus that the tail design should attempt to emulate the SLIP-and-flywheel dynamics. We present four design criteria for a tail which effectively decouples two important control tasks for locomotion, body-pitch control and energy-input. With these criteria, we could make predictions of morphological parameters and analyze the factors limiting tail-use as a system is scaled up in size: in general a long but light tail is best, but as we scale up in size the required mass must also increase. Morphological data on animals is scarce, nonetheless we were able to make some comparisons, which generally seem to match with the predictions.
In the chapter 3 we present a simulation framework with which we applied both particle-swarm optimization algorithms as well as gradient-based algorithms to find open-loop periodic, locally optimal solutions for the models presented in the previous chapter. In comparing different solutions with different parameters, models with parameters that follow our previously derived design criteria result in more optimal solutions, lending weight to our hypothesis. Further, we made a preliminary stability analysis using Floquet analysis, closing the loop by modulating the control-trajectory with the control Jacobian of the return-map. Our initial results indeed showed the longer and lighter tail to be more capable of stabilizing perturbations to body-pitch.
In the chapter 4 we detail the design and construction of a simple 1-DoF tail module for the CheetahCub robot[44]. We ran several tests exploring the effect of different control parameters as well as physical parameters of the tail in generating a bounding gait. In most cases the hind hips provide most of the power, and the landing angle of the hind legs is a very important factor. Using a long and light tail effectively reduces body-pitching as well as renders it much smoother and more stable, as well as resulting in a 25% increase in top speed from $0.4[\frac{m}{s}]$ to $0.5[\frac{m}{s}]$, or from $Fr = 0.125$ to $Fr = 0.196$. Differently from our predictions, when we equip a shorter heavier tail top speed increases by an additional 20% to $0.6[\frac{m}{s}]$ or $Fr = 0.28$. However body-pitching remains the same with the heavier tail. We presume that the increase in performance is due to the ability of using the tail to generate additional momentum, which if timed correctly helps load the springs in the hind-legs and thus obtain better traction. Indeed we observe much less slipping in this case, and the phase-lag between the hind-hips and tail is observed to be an important parameter in tuning.

5.2 Discussion

We have proposed the hypothesis that a tail to be used for steady-state locomotion should be designed in such a way that it simplifies control by decoupling the energy-input and body-pitch stabilization control tasks, with the leg actuators being used for energy-input and tail actuator for stabilization. Alternatively, it is also possible to exploit the coupling and use the tail for energy-input, in addition to the legs[10][22]. Some benefits of this approach are that power requirements can be distributed thus requiring smaller actuators, and the tail is also rather well suited to being fitted with a passive-elastic element to store energy.
It is our opinion that in most cases, decoupling the control tasks and thus simplifying the control problem presents a greater advantage for various reasons. First, from my personal experience in controls both from lectures and in application, being able to deal with separate, single-input-single-output (SISO) systems is simpler by orders of magnitude to dealing with multiple-input-multiple-output systems. Very often, if one simply ignores the weak coupling in a theoretically MIMO system (as we propose to do) and treat the problem as several individual SISO problems, performance can be markedly improved and with much less effort. This because, even though the perturbations to the system are greater (in addition to the outside perturbations are also that which comes from the dynamic couplings), the capability of each individual control loop can be designed in a much more effective manner.
Second, decoupling the control tasks allows all leg-actuators (in particular the hip actuator) to be fully recruited for energy-input. A different way of looking at it is to see the requirements for not causing the body-pitch to start spinning out of control as constraints to leg power output. Indeed, for many cursorial animals (which tend to be hip-powered for running), pitching has been shown to be a greater constraint to maximum running speed[52].
Finally, a recurrent theme in legged-locomotion has indeed been to reduce complexity and move away form a central-program which coordinates and controls the entire system, whether through open-loop control signals such as CPGs[23], decentralized feedback such as reflexes[43][14] or through design of the mechanical dynamics[26][21]. It has been shown that nature often takes this approach, as decerebrate cats[51] and other animals have been shown to be capable of generating complex gaits without any signal from the brain. Our proposed hypothesis fits well with the concept of simplifying control.
From our simuations we have found that models with parameters which followed our proposed design criteria did tend to have lower cost of transport. While this lends some weight to our hypothesis, it should be taken with a grain of salt. Our optimizations yield only locally optimal solutions, and the directions of the gradients is somewhat limited (see subsection 3.1.1). More importantly, these results show a statistical correlation, but not causality: our control inputs are found open-loop without any control rules. A more rigorous approach would be to actually compare the results of different models, in each case using both SISO control loops as well as MIMO control loops, and test their performance not only in terms of efficiency but perhaps more importantly in terms of robustness to perturbations. Indeed, if we compared two designs, one in which the tail and body dynamics are strongly and the other weakly coupled, I would intuitively predict one *with* a high coupling should do better energetically over even terrain, for the reason that peak torques can be reduced by distributing power-load[1]. I expected the advantage in a decoupled-model to more likely be ease of design (both mechanically and of control) and robustness to perturbations.
Nonetheless, most examples we could think of from nature (mostly kangaroos and wallabies of different sizes) seem to also follow the decoupling-approach. From an evolutionary point of view, this approach has another advantage: the simpler, decoupled solution is less sensitive variations and has a wider basin of attraction, making it more "approachable", a necessity for evolution which works by incremental changes[39].
When looking at scaling, we were surprised to find that the limits did not directly originate

[1]Losses in motors scale quadratically with current, which is proportional to torque

from the proposed effectiveness ratios, but indirectly: rapid scaling of the torque-requirements for stabilization (which scale with body mass times a posture-dependent moment-arm) indicate that actuator mass of the tail needs to scale faster the body-mass at $m_T \propto m_B^{\frac{4}{3}}$ (where m_T is tail mass and m_B is body mass), which conflicts with the requirements for decoupling. This led us to also reconsider how well this hypothesis reflects the lower end of the scale, such as in kangaroo-rats or squirrels. Though observations of high-speed videos did show the tail to move in a coordinated manner with the legs, and there have been studies on the necessity of the tail for stability in kangaroo-rats[34][3], whether it is being used actively or not is less evident. If we consider again how rapidly the torque requirements scale, we see that just as they scale very quickly upwards, they also lose importance quickly as we scale down: small animals have much lower inertia to characteristic length[50]. At some point, the requirements become so small that it becomes "easy" for the leg-actuation to control both tasks simultaneously. At this point, the tail can act semi-passively to increase and vary the total MoI: increasing MoI doesn't eliminate body-pitching but it does slow it down, further simplifying the control task for the legs.
In our hardware experiments, we actually had the best results when the coupling was high. An important reason for this is that the robot we used, CheetahCub [44], is extremely light ($\approx 1.25kg$ with tail and head modules) and slips a lot. By using the tail impulse to load the hind-limbs at touch-down, slipping of the hind limbs was greatly reduced. Nonetheless, we found that the long, light tail and the shorter, heavier tail (both with the same MoI) had about the same effect on pitch-stabilization. Thus we believe that these results do not directly conflict our hypothesis; rather, it again indicates that at the lower end of scaling, where gravitational pull is less relevant and thus traction becomes and issue, this hypothesis is less relevant.

5.3 Outlook

I believe that the conclusions of this thesis, i.e. how to design a tail and why, can already be used for designing a future robot. Nonetheless, there are still open questions as well as improvements to be made. On top of this, I feel that both the developed hardware as well as the simulation framework provide a solid starting point from which to do further studies, both on active tails as well as legged locomotion in general. All of this promises a rich outlook.

First and foremost, all control used both in simulation and in hardware was open-loop. How to design a closed-loop control, whether in a conventional engineering or bio-inspired fashion, remains an open -and very interesting- question. Studies on this would also help validate (or discredit) our hypothesis. This can be done both in simulation, with the same framework I used or with a different simulator, as well as in hardware. In hardware it would necessitate either adding sensors to the CheetahCub or making a new tail for a different/new robot. I strongly recommend sensorizing CheetahCub, as I found it to be an excellent platform to work with, both easy and fun to use. Adding even very few and simple sensors, such as touch-sensors to the feet (which was performed at some point, but not yet robustly) and an IMU or even simple gyroscope would open up the possibility of testing many questions in closing the loop with simple decentralized feedback, both with the tail and without.
In the simulation, the optimization tools can be improved. In particular, replacing the truncated Fourier-series of the open-loop control input with a more open and easily optimized trajectory should help in finding better optimal solutions with the gradient-based algorithms. I think combining piece-wise constant steps with the direct-collocation algorithm should prove rather effective. This would also greatly help with the previous suggestion.
Exploring more complicated tail morphology is another obvious direction: we used a simple rigid body with both mass and inertia, however tails in nature are rarely if ever rigid. Kangaroo tails tend to be more rigid than that of most other terrestrial animals, possibly partly because they actually use it as a leg when walking, they are still rather flexible. A semi-flexible tail for the

Cheetah-Cub should be relatively easy to build, although if this path is taken careful consideration should be made as to how to measure and quantify the difference between a rigid and a flexible tail. I suspect that, for passive flexibility the play in the motor-gearing already plays a role.
Finally, I had difficulty in finding biological data that could be readily put into the simulator and compare with my own results. I think it would be both very helpful as well as very interesting to get more comparisons. It would also help us understand actually to what extent scaling does affect the dynamics, and where the boundaries are. The way to go here would be to collaborate with naturalists. Many of them are already using computer simulations and optimization algorithms to validate their own hypotheses [34][20]. I feel that, especially when dealing with dynamics, insight from someone with a grounding in control theory would be of great help to them as well.

Bibliography

[1] R Alexander and Alexandra Vernon. "The mechanics of hopping by kangaroos (Macropodidae)". In: *Journal of Zoology* 177.2 (1975), pp. 265–303.

[2] RMN Alexander. "The gaits of bipedal and quadrupedal animals". In: (1984). DOI: 10.1177/027836498400300205. URL: http://dx.doi.org/10.1177/027836498400300205.

[3] George A Bartholomew and Herbert H Caswell. "Locomotion in kangaroo rats and its adaptive significance". In: *Journal of Mammalogy* (1951), pp. 155–169.

[4] Andrew A Biewener. "Biomechanical consequences of scaling". In: *Journal of Experimental Biology* 208.9 (2005), pp. 1665–1676.

[5] R Blickhan. "The spring-mass model for running and hopping." In: *Journal of biomechanics* 22.11-12 (1989), pp. 1217–1227. DOI: 10.1016/0021-9290(89)90224-8. URL: http://dx.doi.org/10.1016/0021-9290(89)90224-8.

[6] Yvonne Blum et al. "Swing-leg trajectory of running Guinea fowl suggests task-level priority of force regulation rather than disturbance rejection." In: *PloS one* 9.6 (2014). DOI: 10.1371/journal.pone.0100399. URL: http://dx.doi.org/10.1371/journal.pone.0100399.

[7] GA Cavagna, NC Heglund, and CR Taylor. "Mechanical work in terrestrial locomotion: two basic mechanisms for minimizing energy expenditure." In: *The American journal of physiology* 233.5 (1977), R243–R261.

[8] Monica A Daley and Andrew A Biewener. "Running over rough terrain reveals limb control for intrinsic stability." In: *Proceedings of the National Academy of Sciences of the United States of America* 103.42 (2006), pp. 15681–15686. DOI: 10.1073/pnas.0601473103. URL: http://dx.doi.org/10.1073/pnas.0601473103.

[9] Monica A Daley and James R Usherwood. "Two explanations for the compliant running paradox: reduced work of bouncing viscera and increased stability in uneven terrain". In: *Biology letters* 6.3 (2010), pp. 418–421.

[10] Avik De, Aaron M Johnson, and Daniel E Koditschek. "Monopedal Hopping with a Leg and a Tail". In: ().

[11] Russell C Eberhart and Yuhui Shi. "Particle swarm optimization: developments, applications and resources". In: *Evolutionary Computation, 2001. Proceedings of the 2001 Congress on*. Vol. 1. IEEE. 2001, pp. 81–86.

[12] Brian C Fabien. *Analytical system dynamics*. Springer, 2008.

[13] H Geyer, R Blickhan, and A Seyfarth. "Natural dynamics of spring-like running: Emergence of selfstability". In: (2002).

[14] Hartmut Geyer and Hugh Herr. "A muscle-reflex model that encodes principles of legged mechanics produces human walking dynamics and muscle activities." In: *IEEE transactions on neural systems and rehabilitation engineering : a publication of the IEEE Engineering in Medicine and Biology Society* 18.3 (2010), pp. 263–273. DOI: 10.1109/TNSRE.2010.2047592. URL: http://dx.doi.org/10.1109/TNSRE.2010.2047592.

[15] Hartmut Geyer, Andre Seyfarth, and Reinhard Blickhan. "Compliant leg behaviour explains basic dynamics of walking and running." In: *Proceedings. Biological sciences / The Royal Society* 273.1603 (2006), pp. 2861–2867. DOI: 10.1098/rspb.2006.3637. URL: http://dx.doi.org/10.1098/rspb.2006.3637.

[16] Ch. Glocker. "Concepts for modeling impacts without friction". In: *Acta Mechanica* 168 (2004). DOI: 10.1007/s00707-004-0076-3. URL: http://dx.doi.org/10.1007/s00707-004-0076-3.

[17] Christoph Glocker and Christian Studer. "Formulation and Preparation for Numerical Evaluation of Linear Complementarity Systems in Dynamics". In: *Multibody System Dynamics* 13 (2005). DOI: 10.1007/s11044-005-2519-6. URL: http://dx.doi.org/10.1007/s11044-005-2519-6.

[18] Fabian Günther, Fabio Giardina, and Fumiya Iida. "Self-Stable One-Legged Hopping Using a Curved Foot". In: ().

[19] Milton Hildebrand. "Symmetrical gaits of horses". In: *Science* 150.3697 (1965), pp. 701–708.

[20] John R Hutchinson. "Biomechanical modeling and sensitivity analysis of bipedal running ability. I. Extant taxa". In: *Journal of Morphology* 262.1 (2004), pp. 421–440.

[21] F Iida. "Cheap design approach to adaptive behavior: Walking and sensing through body dynamics". In: (2005).

[22] Fumiya Iida et al. "Legged robot locomotion based on free vibration". In: *Advanced Motion Control (AMC), 2012 12th IEEE International Workshop on*. IEEE. 2012, pp. 1–6.

[23] Auke J Ijspeert. "Central pattern generators for locomotion control in animals and robots: a review." In: *Neural networks : the official journal of the International Neural Network Society* 21.4 (2008), pp. 642–653. DOI: 10.1016/j.neunet.2008.03.014. URL: http://dx.doi.org/10.1016/j.neunet.2008.03.014.

[24] AM Johnson et al. "Tail Assisted Dynamic Self Righting: Full Derivations". In: (2012).

[25] Jesse van den Kieboom. "On the dynamics of human locomotion and co-design of lower limb assistive devices". PhD thesis. École Polytechnique FÉdérale de Lausanne, 2014.

[26] TM Kubow and RJ Full. "The role of the mechanical system in control: a hypothesis of self–stabilization in hexapedal runners". In: *Philosophical Transactions of the Royal Society of London. Series B: Biological Sciences* 354.1385 (1999), pp. 849–861.

[27] O'Connor, Shawn M et al. "The kangaroo's tail propels and powers pentapedal locomotion." In: *Biology letters* 10.7 (2014). DOI: 10.1098/rsbl.2014.0381. URL: http://dx.doi.org/10.1098/rsbl.2014.0381.

[28] James H Marden. "Scaling of maximum net force output by motors used for locomotion." In: *The Journal of experimental biology* 208.Pt 9 (2005), pp. 1653–1664. DOI: 10.1242/jeb.01483. URL: http://dx.doi.org/10.1242/jeb.01483.

[29] Etienne-Jules Marey. *La machine animale*. Germer Baillière, 1873.

[30] H-M Maus et al. "Upright human gait did not provide a major mechanical challenge for our ancestors". In: *Nature communications* 1 (2010), p. 70.

[31] Craig P McGowan, J Skinner, and Andrew A Biewener. "Hind limb scaling of kangaroos and wallabies (superfamily Macropodoidea): implications for hopping performance, safety factor and elastic savings". In: *Journal of anatomy* 212.2 (2008), pp. 153–163.

[32] Andreas Merker, Juergen Rummel, and Andre Seyfarth. "Stable walking with asymmetric legs". In: *Bioinspiration & biomimetics* 6.4 (2011), p. 045004.

[33] S Miller, J Van Der Burg, and F Van Der Meché. "Coordination of movements of the hindlimbs and forelimbs in different forms of locomotion in normal and decerebrate cats." In: *Brain research* 91.2 (1975), pp. 217–237. DOI: 10.1016/0006-8993(75)90544-2. URL: http://dx.doi.org/10.1016/0006-8993(75)90544-2.

[34] Jared Moore et al. "Exploring the Role of the Tail in Bipedal Hopping through Computational Evolution". In: *Advances in Artificial Life, ECAL*. Vol. 12. 2013, pp. 11–18.

[35] Katta G Murty and Feng-Tien Yu. *Linear complementarity, linear and nonlinear programming*. Citeseer, 1988.

[36] null and null. "ZERO-MOMENT POINT — THIRTY FIVE YEARS OF ITS LIFE". In: *International Journal of Humanoid Robotics* 01.01 (2004). DOI: 10.1142/S0219843604000083. URL: http://dx.doi.org/10.1142/S0219843604000083.

[37] null, null, and null. "The use of compliant joints and elastic energy storage in bio-inspired legged robots". In: *Mechanism and Machine Theory* 44.3 (2009). DOI: 10.1016/j.mechmachtheory.2008.08.010. URL: http://dx.doi.org/10.1016/j.mechmachtheory.2008.08.010.

[38] Dai Owaki and Akio Ishiguro. "Enhancing stability of a passive dynamic running biped by exploiting a nonlinear spring". In: *Intelligent Robots and Systems, 2006 IEEE/RSJ International Conference on*. IEEE. 2006, pp. 4923–4928.

[39] Rolf Pfeifer, Josh Bongard, and Simon Grand. *How the body shapes the way we think: a new view of intelligence*. MIT press, 2007.

[40] Marc H Raibert et al. *Legged robots that balance*. Vol. 3. MIT press Cambridge, MA, 1986.

[41] C David Remy, Keith Buffinton, and Roland Siegwart. "A matlab framework for efficient gait creation". In: (2011), pp. 190–196.

[42] Jonas Rubenson et al. "Reappraisal of the comparative cost of human locomotion using gait-specific allometric analyses". In: *The Journal of experimental biology* 210.20 (2007), pp. 3513–3524.

[43] Joseph C Spagna et al. "Distributed mechanical feedback in arthropods and robots simplifies control of rapid running on challenging terrain". In: *Bioinspiration & biomimetics* 2.1 (2007), p. 9.

[44] A. Sprowitz et al. "Towards dynamic trot gait locomotion: Design, control, and experiments with Cheetah-cub, a compliant quadruped robot". In: *The International Journal of Robotics Research* 32 (2013). DOI: 10.1177/0278364913489205. URL: http://dx.doi.org/10.1177/0278364913489205.

[45] Dipl Math Oskar von Stryk. *Numerical solution of optimal control problems by direct collocation*. Springer, 1993.

[46] McMahon, TA. "Using body size to understand the structural design of animals: quadrupedal locomotion." In: *Journal of applied physiology* 39.4 (1975), pp. 619–627.

[47] Vance A Tucker. "Energetic cost of locomotion in animals". In: *Comparative Biochemistry and Physiology* 34.4 (1970), pp. 841–846.

[48] Jesse Van Den Kieboom, Soha Pouya, and Auke Jan Ijspeert. "Meta Morphic Particle Swarm Optimization". In: *Nature Inspired Cooperative Strategies for Optimization (NICSO 2013)*. Springer, 2014, pp. 231–244.

[49] Christopher L Vaughan and Mark J O'Malley. "Froude and the contribution of naval architecture to our understanding of bipedal locomotion". In: *Gait & posture* 21.3 (2005), pp. 350–362.

[50] Steven Vogel. *Cats' paws and catapults: Mechanical worlds of nature and people*. WW Norton & Company, 2000.

[51] PJ Whelan. "Control of locomotion in the decerebrate cat." In: *Progress in neurobiology* 49.5 (1996), pp. 481–515. DOI: 10.1016/0301-0082(96)00028-7. URL: http://dx.doi.org/10.1016/0301-0082(96)00028-7.

[52] Sarah B Williams et al. "Pitch then power: limitations to acceleration in quadrupeds." In: *Biology letters* 5.5 (2009), pp. 610–613. DOI: 10.1098/rsbl.2009.0360. URL: http://dx.doi.org/10.1098/rsbl.2009.0360.